

**DEVELOPMENT OF A MATHEMATICAL MODEL TO PREDICT  
ELECTROMAGNETIC INTERFERENCE IN AUTOMOTIVE DATA  
COMMUNICATION STRUCTURE**

**by**

**Tamer A. Taher**

**Submitted in Partial Fulfillment of the Requirements**

**for the Degree of**

**Master of Science in Engineering**

**in the**

**Electrical and Computer Engineering**

**Program**

**YOUNGSTOWN STATE UNIVERSITY**

**December, 2006**

# Development of a Mathematical Model to Predict Electromagnetic Interference in Automotive Data Communication Structure

Tamer A. Taher

I hereby release this thesis to the public. I understand that this thesis will be made available from the OhioLINK ETD Center and the Maag library Circulation Desk for public access. I also authorize the University or other individuals to make copies of this thesis as needed for scholarly research.

Signature:



Tamer A. Taher, Student

Dec 11, 2006

Date

Approvals:



Dr. Jalal Jalali, Thesis Advisor

12/11/2006

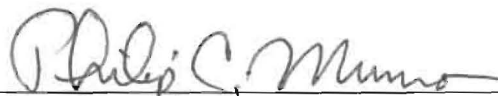
Date



Dr. Frank X. Li, Committee Member

12/11/2006

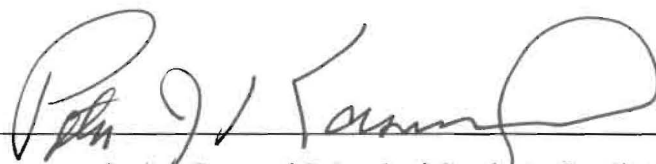
Date



Dr. Philip C. Munro, Committee Member

11-Dec-2006

Date



Peter J. Kasvinsky, Dean of School of Graduate Studies & Research

12/14/06

Date



## ABSTRACT

A model is designed to predict the electromagnetic interference noise from adjacent circuits. Experimental results are obtained for three Rip Cord cables and compared with predictions of the multi conductor transmission line models. Based on the experimental configurations tested, it appears that accurate predictions of crosstalk-coupling can be achieved in these controlled-characteristic cables.

The prediction is accurate for high frequencies (i.e. 80 MHz) where the lines are electrically long or for low frequencies (i.e. 100 kHz) where the lines are electrically short. Typical applications are circuits of  $n$  wires,  $n$  wires above a ground plane, UTP (unshielded twisted pair), STP (shielded twisted pair), and coaxial cables.

*To the world*

# TABLE OF CONTENTS

ABSTRACT .....	III
DEDICATION .....	V
TABLE OF CONTENTS .....	V
LIST OF FIGURES.....	VII
LIST OF SYMBOLS.....	IX
<b>CHAPTER ONE</b>	
INTRODUCTION .....	1
<b>CHAPTER TWO</b>	
CIRCUIT HIGH FREQUENCY BEHAVIOR .....	3
2.1 WIRES.....	4
2.2 RESISTORS .....	5
2.3 CAPACITORS .....	6
2.4 INDUCTORS .....	7
<b>CHAPTER THREE</b>	
COUPLING MECHANISMS.....	8
3.1 CAPACITIVE COUPLING.....	8
3.1.1 <i>Three Cables (Including Experiment)</i> .....	9
3.2 INDUCTIVE COUPLING.....	14
3.2.1 <i>Three Cables</i> .....	15
<b>CHAPTER FOUR</b>	
4.1 METHOD 1: MATRIX DEFINITION .....	22
4.2 METHOD 2: WIDE SEPARATION APPROXIMATIONS .....	24
4.3 METHOD 3: NUMERICAL METHODS .....	27
<b>CHAPTER FIVE</b>	
MATHEMATICAL MODEL.....	30
5.1 GENERAL N WIRES EQUATIONS: .....	30
5.1.1 <i>Method 1: Definition</i> .....	32
5.1.2 <i>Method 2: Similarity Transformation</i> .....	33
5.1.3 <i>Method 3: Hyperbolic Function</i> .....	34

5.1.4 Method 4: Ideal Case.....	35
5.2 THE TERMINAL CONSTRAINTS .....	36
<b>CHAPTER SIX</b>	
<b>THREE RIP CORD CABLES</b>	
6.1 EXPERIMENT SETUP.....	43
6.2 MODEL VERSUS MEASUREMENTS .....	45
6.2 MODEL VERSUS MEASUREMENTS .....	46
6.2.1 Basic Configuration.....	47
6.2.2 Changing Voltage Source Noise .....	52
6.2.3 Changing Wires Length.....	54
6.2.4 Changing Load Impedance .....	57
6.2.5 Changing Separation between Wires.....	59
<b>CHAPTER SEVEN</b>	
<b>CONCLUSION .....</b>	<b>63</b>
<b>APPENDIX A</b>	
<b>MATLAB SOURCE CODE.....</b>	<b>65</b>
<b>REFERENCES .....</b>	<b>69</b>

## LIST OF FIGURES

Figure 1	Data transmission lines.	2
Figure 2	The skin effect in a wire.	4
Figure 3	Equivalent circuit of a resistor (high frequency).	6
Figure 4	Equivalent circuit of a capacitor (high frequency).	6
Figure 5	Equivalent circuit of an inductor (high frequency).	7
Figure 6	Representation of two cables, (a) physical representation, (b) capacitive coupling, (c) equivalent circuit looking from the victim side.	9
Figure 7	Experiment: (a) near wire monitoring, (b) far wire monitoring.	10
Figure 8	Physical representation, (a) near cable, (b) far cable.	11
Figure 9	Equivalent circuit, (a) near cable (b) far cable.	12
Figure 10	Reduced equivalent circuit, (a) near cable (b) far cable.	13
Figure 11	Inductive coupling, (a) physical representation, (b) equivalent circuit.	14
Figure 12	Inductive coupling between three cables.	15
Figure 13	Inductive coupling between three wires, (a) the setup of far cable, (b) equivalent circuit.	16
Figure 14	Inductive coupling between three wires, (a) the setup of near cable, (b) equivalent circuit.	18
Figure 15	Examples of multi-transmission lines.	19
Figure 16	The per unit length parameters.	20
Figure 17	Magnetic flux per unit length of a wire.	24
Figure 18	Charge distribution, (a) unit length distribution, (b) voltage between two points.	25
Figure 19	Two wires with $s$ as separation.	26
Figure 20	Three wires configuration.	27
Figure 21	Method of Moments.	28
Figure 22	Terminal Networks.	36
Figure 23	Cross section of Rip Cord wires, (a) one wire, (b) two wires.	38
Figure 24	Parameters per unit length of three Rip Cords.	39

Figure 25	Three Rip Cords connection inside a circuit.	39
Figure 26	NoiseKen tent.	43
Figure 27	Test setup.	43
Figure 28	VEE Pro.	44
Figure 29	Physical representation of test setup.	45
Figure 30	Three dimensions of test setup.	45
Figure 31	Three Rip Cords terminal conditions.	46
Figure 32	Basic configuration, sample A.	49
Figure 33	Basic configuration, sample B.	50
Figure 34	Basic configuration, sample C.	51
Figure 35	Changing voltage source noise to 5 volts peak to peak.	53
Figure 36	Changing wires length to 1.0 meter, sample A.	55
Figure 37	Changing wires length to 1.0 meter, sample B.	56
Figure 38	Changing Load Impedance to 9.851 k $\Omega$ .	58
Figure 39	Changing separation between wires to 1 cm (398.3 mils), sample A.	61
Figure 40	Changing separation between wires to 1 cm (398.3 mils), sample B.	62
Figure 41	Multi-transmission lines examples, (a) n wires above a ground plane, (b) untwisted shielded pair.	64

# LIST OF SYMBOLS

$R_{DC}$	DC resistance
$\delta$	Skin depth
$L_{\text{internal}}$	Internal inductance
$L_{\text{external}}$	External inductance
C2	Lead capacitance
C1	Capacitance that represents a certain charge separation effect
Rx	Dielectric insulation resistance
Ry	Series resistance
Cx	Coupling capacitance between conductors
Cy, Cz	Capacitance between conductor and the ground
$M$	External inductance or mutual inductance
$\sigma$	Conductivity
$\varepsilon$	Permittivity
$\mu$	Permeability
$\bar{V}(z,t)$	Voltage matrix at z in the time domain
$\bar{I}(z,t)$	Current matrix at z in the time domain
$\bar{L}$	Inductance matrix, per unit length parameters
$\bar{C}$	Capacitance matrix, per unit length parameters
$\bar{R}$	Resistance matrix, per unit length parameters
$\bar{G}$	Conductance matrix, per unit length parameters
$1_n$	Identity matrix
$\bar{\Psi}$	$n \times 1$ matrix containing the total magnetic flux per unit length $\Psi_i$ penetrating the i-th circuit which is defined between the i-th line and the reference line
$l_{ii}$	Inductance with respect to the ground- self inducting

$l_{ij}$	Mutual inductance between two conductors
$\overline{Q}$	$n \times 1$ matrix containing the total charge per unit length on the $i$ -th conductor as $q_i$ ,
$c_{ii}$	Capacitance with respect to the ground- self inducting
$c_{ij}$	Mutual capacitance between two conductors
$\xi$	Transverse magnetic field intensity
$\phi_{12}$	Magnetic flux from current 1 to wire 2
$E$	Electric field
$r$	Wire radius
$s$	Cross section area
$\alpha_i$	Charge over each sub area
$R_{ij}$	Distance between the sub areas bearing the unknown charge
$\hat{V}(z)$	Voltage matrix at $z$ in phosor form
$\hat{I}(z)$	Current matrix at $z$ in phosor form
$\hat{Z}$	Impedance matrix in phosor form
$\hat{Y}$	Admittance matrix in phosor form
$\hat{\Phi}(\lambda)$	Chain parameter matrix in phosor form
$\hat{Z}_c$	Characteristic impedance matrix in phosor form
$\hat{Y}_c$	Characteristic admittance matrix in phosor form
$\hat{\gamma}$	Propagation constant matrix in phosor form
$Z_s$	Generator source impedance
$Z_\lambda$	Generator load impedance
$Z_{FE}$	Receptor load impedance
$Z_{NE}$	Receptor source impedance
$V_s$	Generator voltage source
$c_M$	Mutual capacitance between receptor and generator



$c_R$	Capacitance of the receptor with reference to ground
$c_G$	Capacitance of the generator with reference to ground
$l_M$	Mutual inductance between receptor and generator
$l_R$	Inductance of the receptor with reference to ground
$l_G$	Inductance of the generator with reference to ground
$\lambda$	Wire length
$\hat{V}_R(\lambda)$	Voltage across the load impedance in the receptor circuit in phosor form
$V_{FE}$	Voltage far end, voltage across the load impedance in the receptor circuit in phosor form
$\hat{V}_R(0)$	Voltage across the source impedance in the receptor circuit in phosor form
$V_{NE}$	Voltage near end, voltage across the source impedance in the receptor circuit in phosor form

# CHAPTER ONE

## INTRODUCTION

One of the primary requirements for vehicles (automobiles and trucks) is to be dependent on electronics for their performance, or in other words, to be controlled by high frequency data communication structure. Hence they are becoming increasingly susceptible to external electromagnetic emissions and are becoming sources of electromagnetic emissions. In order to ensure that these electronics or data communication structure will not be interfered with or cause interference among themselves or with external receptors, a procedure is needed to be established to ensure that the data cable structures are best suited for their intended use in the vehicle network.

This thesis concerns the analysis and prediction of data communication structure at both low and high frequency. The analysis depends on the ability of data communication structure which is electromagnetic emission to cause interference in electrical and electronic devices. This kind of interference can cause one of the circuits to function properly or may damage the whole circuit. One of the main factors that should be taken into consideration is frequency; due to the fact that at high frequency the interference will be the major influence [1].

Communications between circuits will be affected by electromagnetic interference, which is caused by data transmission line coupling. Figure 1 illustrates the main problem. The interference happens between all data transmission lines. In order to obtain a complete solution for the interference between the lines, we need to understand the behavior of circuits at high frequency which will be discussed in chapter 2. After that we discuss the concept of coupling in chapter 3. Chapter 4, parameters per unit length for data transmission line, will discuss methods to find the parameters per unit length-data transmission lines and how these methods can be applied. The solutions to multi-data transmission lines and finding the interference will be presented in chapter 5, multi-transmission lines. In chapter 6, three Rib Cord wires are analyzed and tested. Finally, in

chapter 7, conclusion is provided, a picture of what can be done in the future, and ways to do it are also provided.

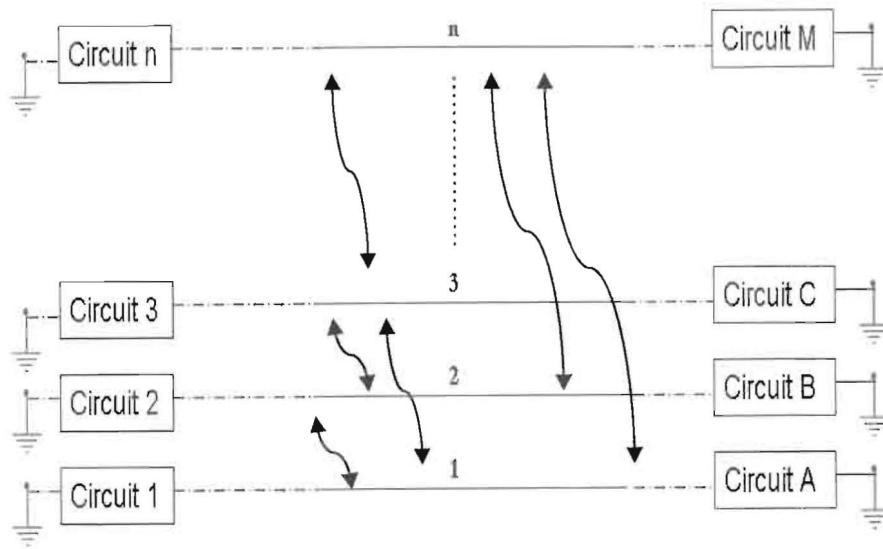


Figure 1: Data transmission lines.

## CHAPTER TWO

### CIRCUIT HIGH FREQUENCY BEHAVIOR

Circuit components vary with frequency. Since actual components are not ideal, their characteristics and impedance deviate from those of the theoretical components. In this chapter we discuss the typical circuit components and how the component characteristics vary with frequency since there are several major differences between signals at high frequency and their counterparts at low frequency or even DC (direct current). Wire, resistance, capacitance, and inductance are our interest here.

Before going further, the question of whether a circuit or discrete component has to be treated in high or low frequency should be discussed [2]. The transition from low frequency analysis like Kirchhoff's laws to high frequency treatment involving voltage and current waves depends on signal wavelength in comparison with the maximum size of the circuit or discrete component. The transition takes place gradually as the signal wavelength becomes increasingly comparable with the circuit or the discrete component. As a rule of thumb, when the maximum length of circuit is more than 1/10 of the signal wavelength, high frequency theories should be taken into consideration since the low frequency rules do not apply. This is written as:

$$\begin{aligned} \lambda > \frac{\lambda}{10} & : \text{High frequencies behavior should be taken} \\ & \text{in consideration} \\ \lambda < \frac{\lambda}{10} & : \text{Low frequencies behavior can be applied} \\ & \text{such as Kirchhoff's laws} \end{aligned} \tag{2.1}$$

where  $\lambda$  is the maximum length of circuit, and  $\lambda$  is the wavelength of the frequency of interest.

## 2.1 Wires

Normally, wires or conductors are not considered as a component; however, at high frequency, wire acts as an inductor. As an example, if a pair of lines or conductors is electrically long for the frequency of operation, then we should deal with them as transmission line. On the other side, if a pair is electrically short, then the normal model (short circuit) for wires at low frequency should be taken in consideration.

Usually, the behavior of a conductor depends on the length and cross section area or radius of cross section area of the conductor. To standardize the wires, the American Wire Gauge (AWG) system is used widely. In this system, the diameter of a wire will roughly double for every six gauges. There are two main factors that influence the behavior of a conductor: skin effect and inductance [3].

The electrical signals propagate less inside the conductor as frequency increases, at the same time, the current density increases near the outside perimeter as shown in figure 2[3]. This effect is known as the skin effect. For instance, a copper wire of radius  $r$ , length  $\lambda$ , and conductivity  $\sigma$  has a DC resistance of:

$$R_{DC} = \frac{\lambda}{\pi r^2 \sigma_{cond}} \quad (2.2)$$

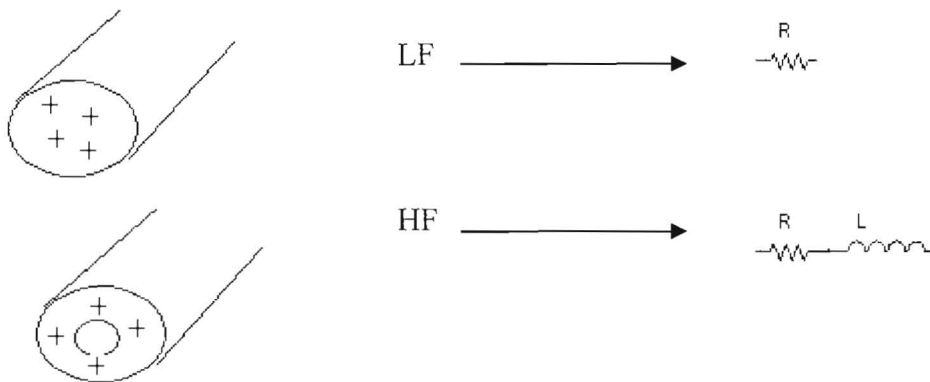


Figure 2: The skin effect in a wire.

The skin depth is:

$$\delta = \frac{1}{\sqrt{\pi f \mu_0 \sigma_{cond}}} \quad (2.3)$$

Further calculations reveal normalized resistance under high frequency is:

$$R \cong R_{DC} \frac{r}{(2\delta)} \cong \frac{\lambda}{2r} \sqrt{\frac{\mu_0 f}{\sigma \pi}} \quad (2.4)$$

The internal inductance usually is negligible compared to the external inductance. The internal inductance is further reduced when higher frequency currents are considered. The DC internal inductance ( $L_{internal}$ ) is derived as [4]:

$$L_{internal} = \frac{\lambda \mu_0}{8 \pi} \quad \text{For low frequency} \quad (2.5)$$

The current will tend toward the surface as frequency increased (high frequency); the high frequency internal inductance is derived as [5]:

$$L_{internal} = \frac{2 \delta L_{internal}}{r} \cong \frac{\lambda}{4 \pi r} \sqrt{\frac{\mu_0}{\sigma f \pi}} \quad (2.6)$$

For two parallel conductors carrying uniform current in opposite directions and running in free space with  $D$  as center-to-center spacing, and  $d$  as the wire diameter, the external inductance is derived as [1]:

$$L_{external} = 0.01 \times 10^{-6} \lambda \ln \frac{2D}{d} \quad (2.7)$$

## 2.2 Resistors

One of the most common circuit elements in electronics is a resistor. It can take on many forms such as

- Thin film type
- Composition or carbon resistors
- Wire wound

Resistors behave differently at low frequencies than high frequencies. At low frequency  $V \approx R I$ , where  $R$  is the resistor,  $I$  is the current through the resistor, and  $V$  is the voltage across the resistor. On the other hand,  $V \neq R I$  at high frequency. The

ideal frequency response of a resistor has a magnitude equal to the value of the resistor and a phase angle of 0 degrees [3].

At high frequency, the equivalent circuit representation of a resistor of value  $R$  is shown in figure 3. The representation takes into account the finite lead length as well as parasitic capacitance  $C1$  is the capacitance that represents a certain charge separation effect, while  $C2$  is the lead capacitance [6].

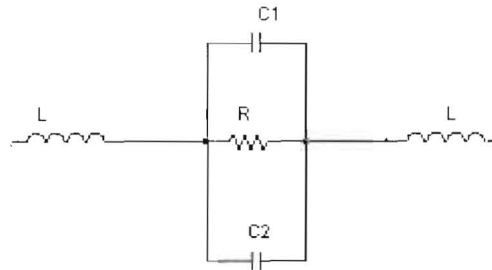


Figure 3: Equivalent circuit of a resistor (high frequency).

## 2.3 Capacitors

The behavior of a capacitor is dependent on its dielectric; for a parallel plate capacitor, designers define capacitance with the assumption that the separation between the plates is much smaller than the area as:

$$C = \epsilon \frac{A}{d} \quad (2.8)$$

where  $\epsilon$  is the permittivity for the dielectric between the plates,  $A$  is the cross section area between the plates, and  $d$  is the separation between the plates. The frequency response of an ideal capacitor is defined as [7]:

$$\hat{Z} = \frac{1}{j\omega C} = \frac{1}{j\omega C} \angle -90^\circ \quad (2.9)$$

The equivalent circuit for a real capacitor in high frequency is shown in figure 4, where  $R_x$  is the dielectric insulation resistance,  $R_y$  is the series resistance,  $L$  is the inductance that has been generated by the leads, and  $C$  is the actual capacitance.

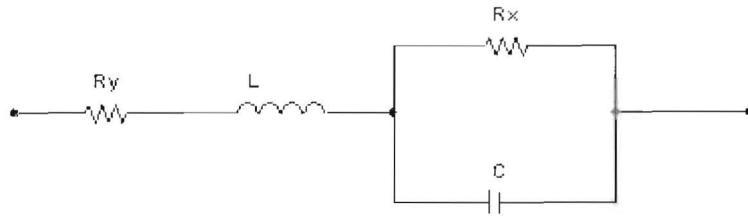


Figure 4: Equivalent circuit of a capacitor (high frequency).

## 2.4 Inductors

Inductors can be used in many applications such as filters, shifters, and microwave circuits. The response of an ideal inductor is [7]:

$$\hat{Z} = j\omega L = \omega L \angle 90^\circ \quad (2.10)$$

The equivalent circuit for a real inductor at high frequency is shown in figure 5, where  $C_y$  is the distributed shunt capacitance,  $R_x$  represents the internal series resistance of the inductor and the shunt resistance between turns, and  $L$  is the actual inductor.

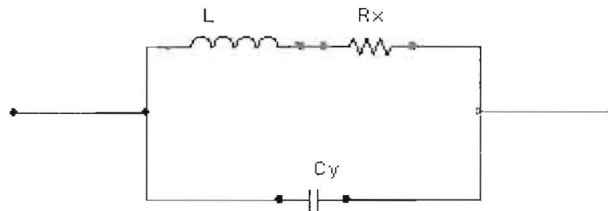


Figure 5: Equivalent circuit of an inductor (high frequency).



# CHAPTER THREE

## COUPLING MECHANISMS

This chapter covers the coupling mechanisms that occur between cables. For simplicity, we are going to assume that the coupling between cables is weak; therefore the victim cable is not coupling back to the source cable.

Two types of coupling are discussed in this chapter; capacitive coupling and inductive coupling. Capacitive coupling and inductive coupling occur simultaneously, and it is not easy to distinguish between them. For simplicity, if we connect the source circuit to an open load (i.e.  $10\text{ M}\Omega$ ), the current will be almost zero, and the voltage will be same as the source voltage along the source cable, which will turn capacitive coupling to maximum influence and the inductive coupling to almost zero influence. On the other hand, if we connect the source circuit to a short load (i.e.  $1\ \Omega$ ), the current will be very large along the source cable, and the voltage difference along the source cable will be almost zero, which will turn inductive coupling to maximum influence and the capacitive coupling to almost zero influence [7].

### 3.1 Capacitive Coupling

Figure 6 shows a simple representation of a capacitive coupling between two conductors.  $C_x$  is the coupling capacitance between conductor 1 and 2,  $C_y$  is the capacitance between conductor 1 and the ground, and  $C_z$  is the capacitance between conductor 2 and the ground. The output voltage at the R is given by:

$$V_r / V = \frac{j\omega \frac{C_x}{(C_x + C_z)}}{j\omega + \frac{1}{R(C_x + C_z)}} \quad (3.1)$$

Capacitance  $C_x$  can be decreased or increased by proper orientation of the cables (increasing or decreasing the distance between the cables).

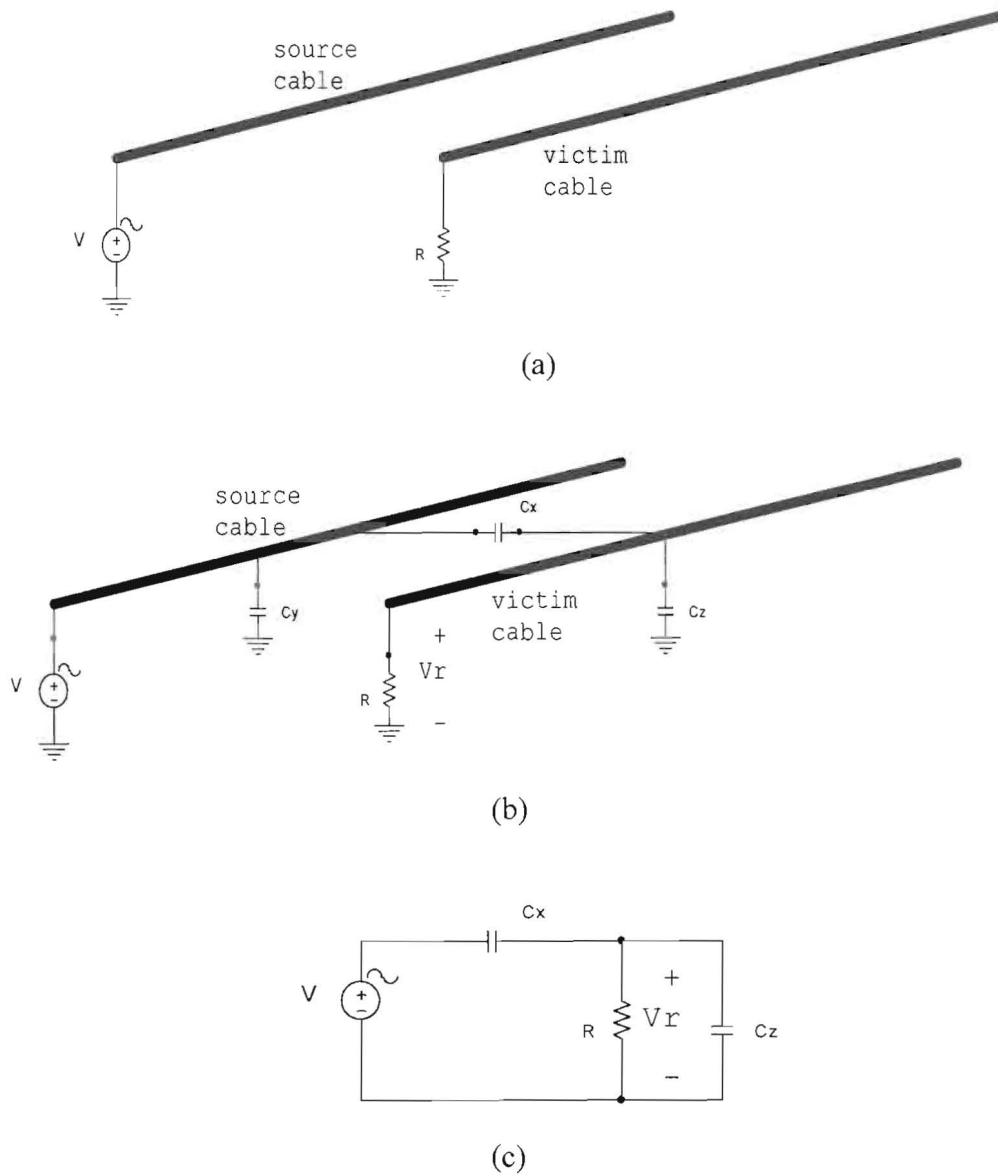
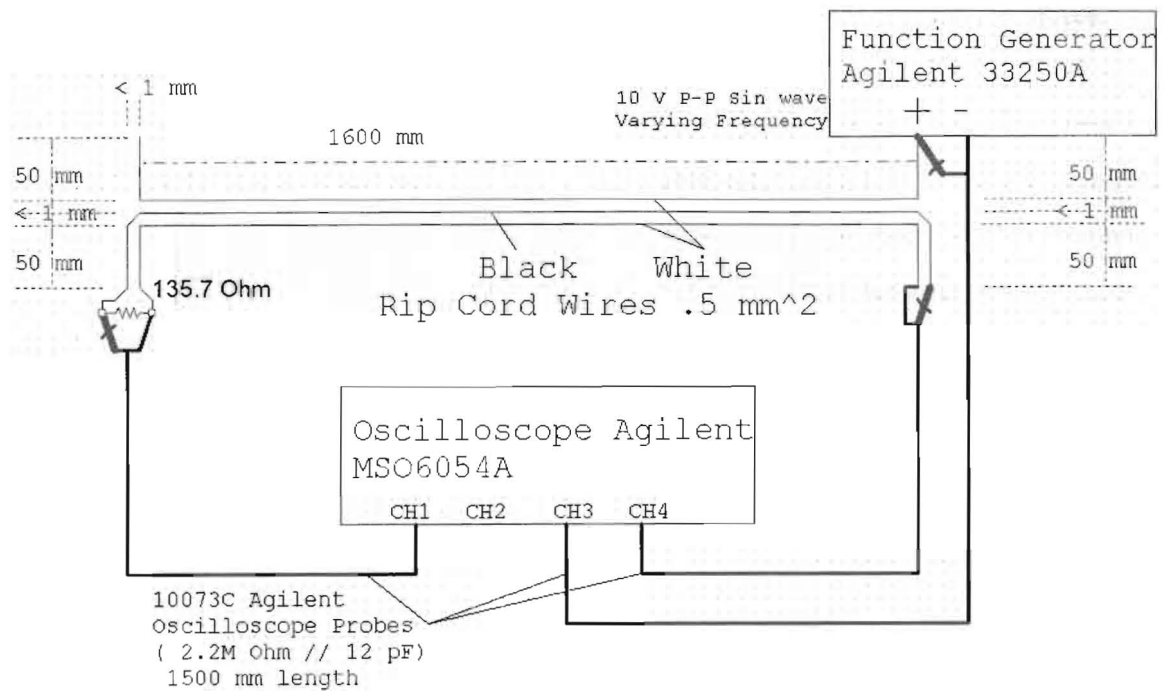


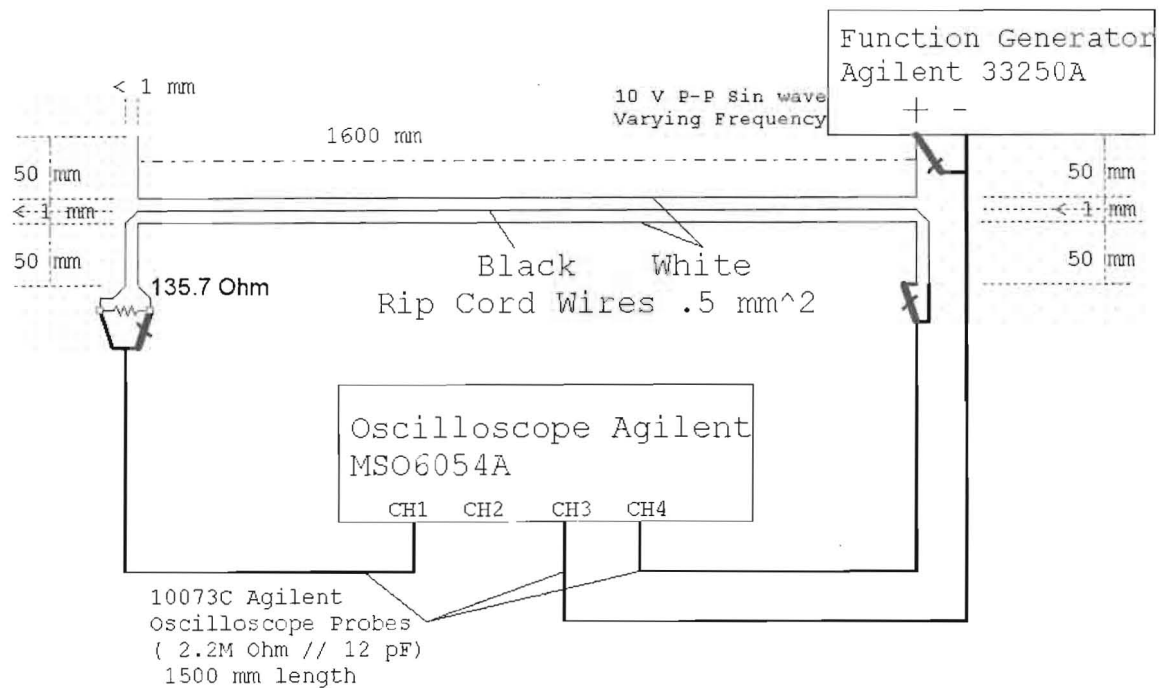
Figure 6: Representation of two cables, (a) physical representation, (b) capacitive coupling, (c) equivalent circuit looking from the victim side.

### 3.1.1 Three Cables (Including Experiment)

The following experiments were performed to test the capacitive coupling for three cables as shown in figure 7(a, b). The difference between near wire monitoring (near end) and far wire monitoring (far end) is the reference cable. In near wire the reference is the bottom cable, while in the far end the reference is the middle cable.



(a)



(b)

Figure 7 Experiment: (a) near wire monitoring, (b) far wire monitoring.

A simple representation can be shown in figure 8 for both near and far cables. The equivalent circuits for both configurations become those of figure 9(a, b). The reduced equivalent circuits for both configurations are shown in figure 10(a, b), where  $C1$  is the distributed capacitance between the source cable and far cable,  $C2$  is the distributed capacitance between the source cable and the near cable,  $C3$  is the distributed capacitance between far cable and near cable,  $G1=1/R1$  is the shunt resistance between source cable and far cable,  $G2 =1/R2$  is the shunt resistance between source cable and near cable,  $G3 =1/R3$  is the shunt resistance between the far cable and near cable, and the 12pF parallel with 2.2 M  $\Omega$  is the input impedance for combination of probe and oscilloscope.

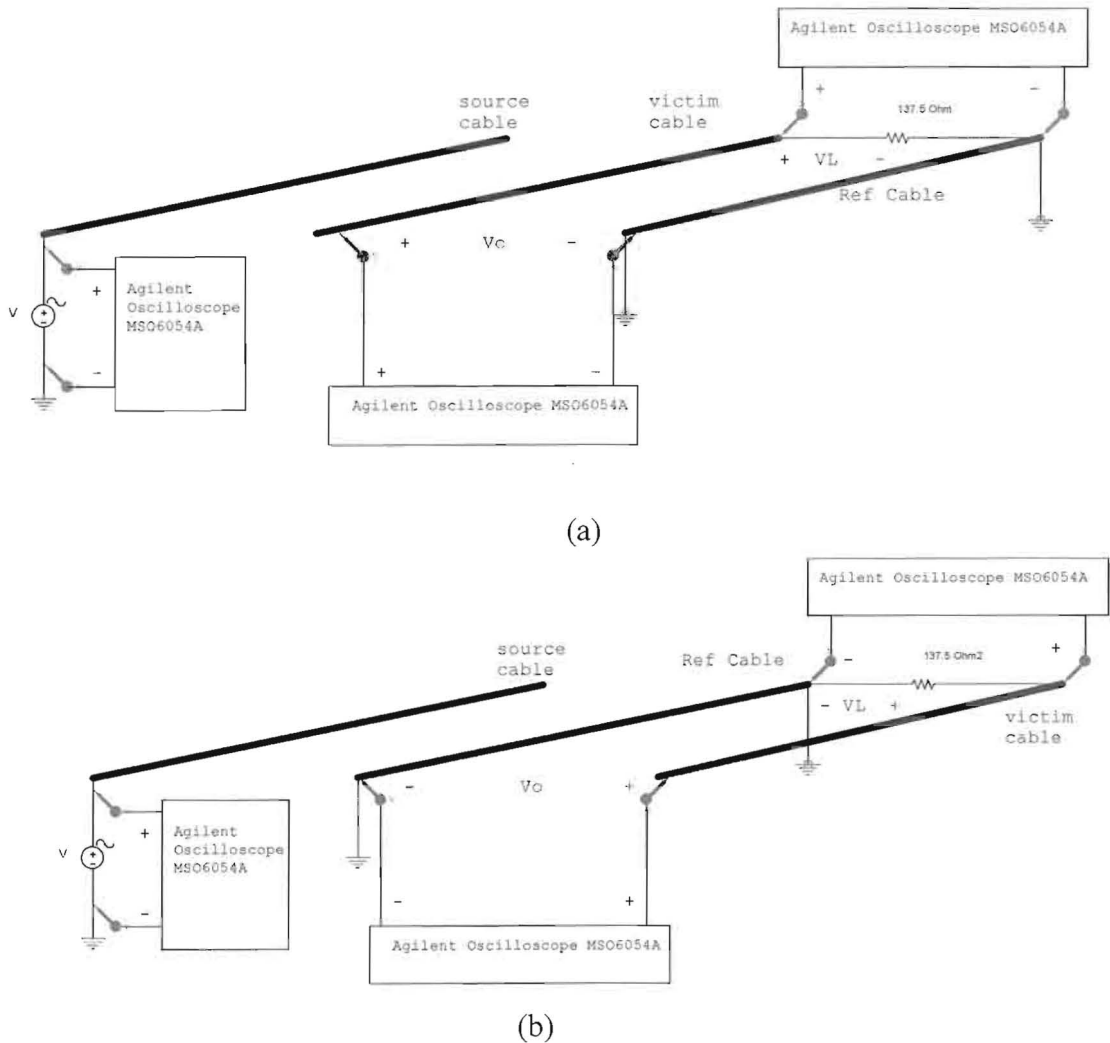
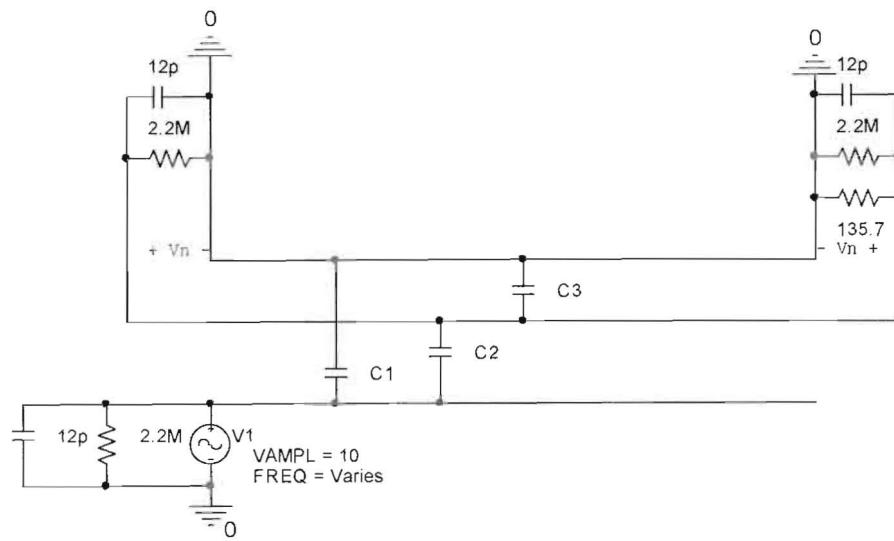
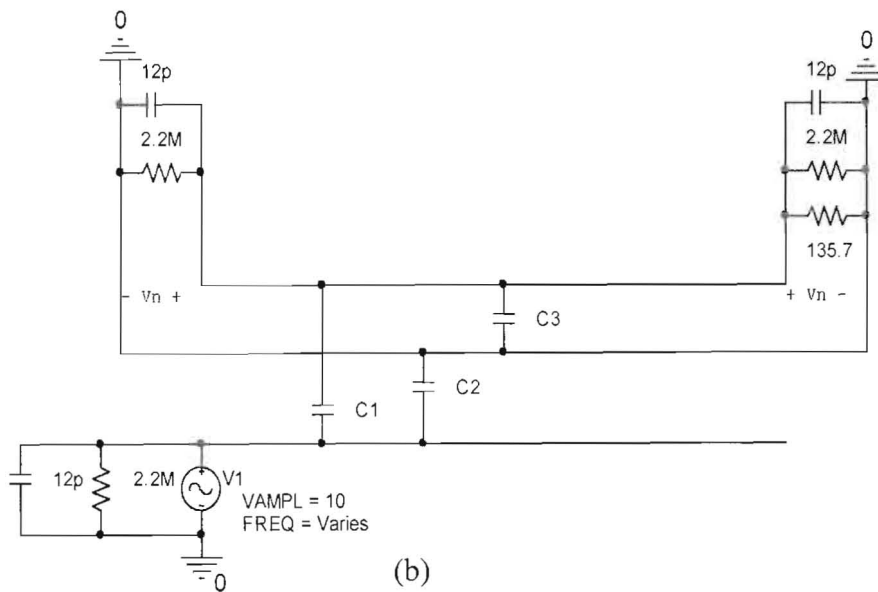


Figure 8: Physical representation, (a) near cable, (b) far cable.

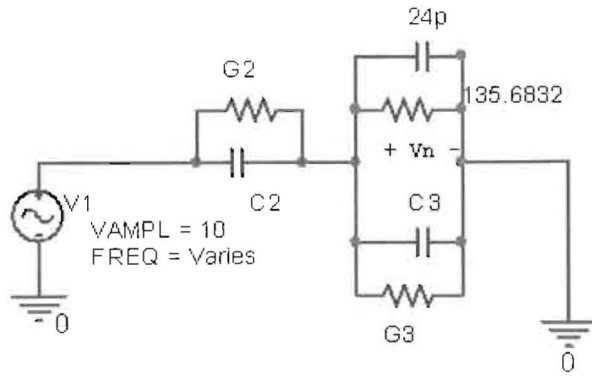


(a)

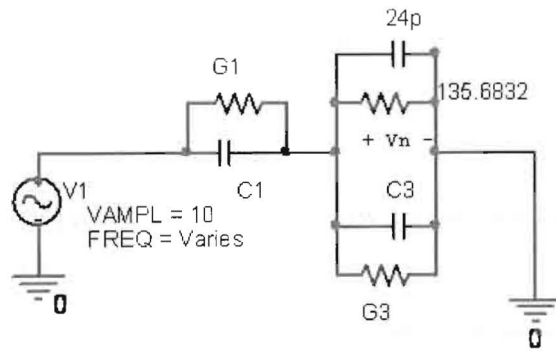


(b)

Figure 9: Equivalent circuit, (a) near cable (b) far cable.



(a)



(b)

Figure 10: Reduced equivalent circuit, (a) near cable (b) far cable.

The voltage  $V_n$  at both end of the near configuration circuit is:

$$V_n = \frac{G_2 + j\omega C_2}{\frac{1}{135.6823} + j\omega 24p + 2(G_2 + j\omega C_2)} V_1 \quad (3.3)$$

This can be reduced to:

$$G_2 + j\omega C_2 = \frac{\frac{1}{135.6823} + j\omega 24p}{\frac{V_n}{V_1} - 2} \quad (3.4)$$

The voltage  $V_n$  at both end of the far configuration circuit is:

$$V_n = \frac{G_1 + j\omega C_1}{G_2 + G_1 + \frac{1}{135.6823} + j\omega(24p + C_3 + C_1)} V_1 \quad (3.5)$$

This can be reduced to:

$$G_1 + j\omega C_1 = \frac{G_2 + \frac{1}{135.6823} + j\omega(24p + C_3)}{\frac{V_n}{V_1} - 1} \quad (3.6)$$

### 3.2 Inductive Coupling

The mutual inductance or external inductance  $M$  is produced when current  $I$  flows in one circuit and produces a flux  $\phi_{12}$  in the second circuit:

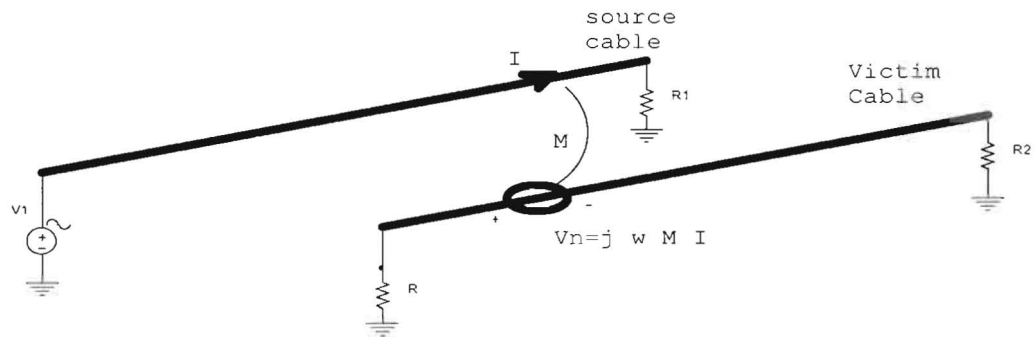
$$M = \frac{\phi_{12}}{I} \quad (3.7)$$

The induced voltage  $V_n$  can be derived using Faraday's law and reduced to be [8],

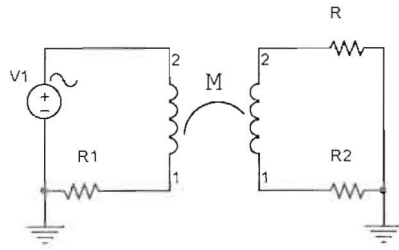
$$V_n = j\omega B A \cos\theta = j\omega M I \quad (3.8)$$

where  $B$  is the flux density, and  $A$  is the area of the closed loop with respect to ground.

The circuit equivalent of inductive coupling is shown in figure 11(a, b).



(a)



(b)

Figure 11: Inductive coupling, (a) physical representation, (b) equivalent circuit.

### 3.2.1 Three Cables

The block diagram for three cables under inductive coupling is shown in figure 12. From section 3.1.1, in order to test inductive coupling, the experiment needs to be changed. We need to connect a small resistance at the end of the source cable. This can be illustrated in figure 13 and figure 14.

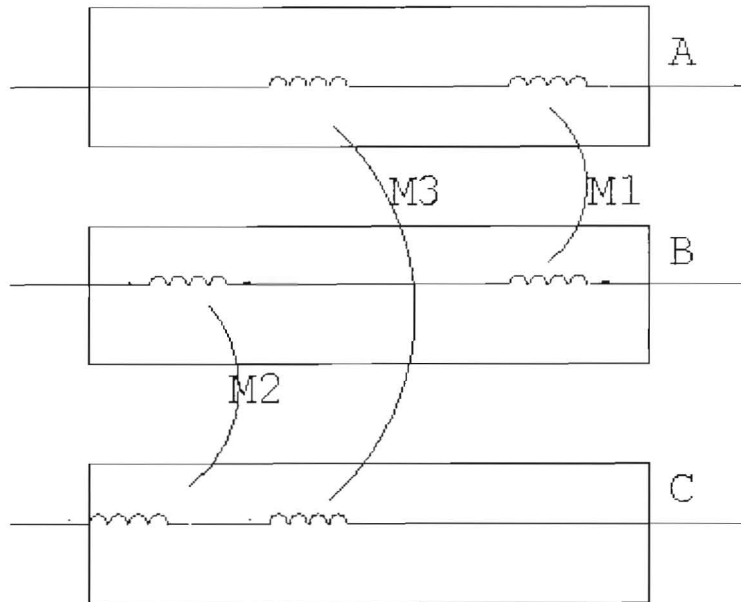


Figure 12: Inductive coupling between three cables.



Again, the difference between near wire monitoring (near end) and far wire monitoring (far end) is the reference cable. In near wire, the reference is the bottom cable, while in the far end; the reference is the middle cable. In near wire, we are interested in measuring the induced voltage at the middle victim cable. On the other hand, in the far cable, we are interested in measuring the induced voltage at the far victim cable as shown in figure 8 [5].

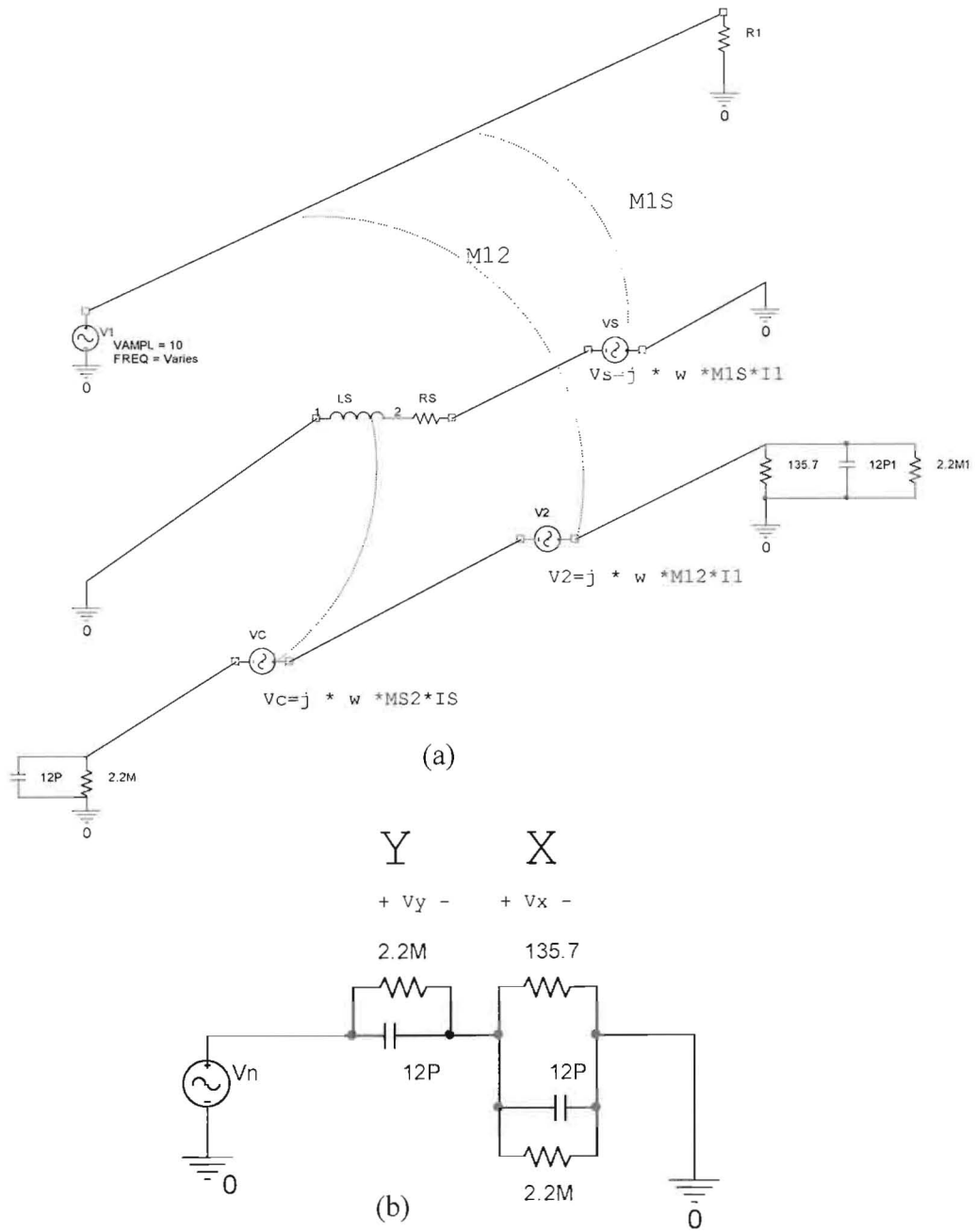


Figure 13: Inductive coupling between three wires, (a) the setup of far cable, (b) equivalent circuit.

The simplified equations for the above configuration are:

$$V_n = \frac{j\omega(M_{12} R_s + j\omega M_s (M_{12} - M_s)) V_1}{R_s + j\omega M_s} \frac{V_1}{R_1} \quad (3.9)$$

X is the total impedance at the right while y is the total impedance at the left as shown in figure 13.

$$X = 135.69 // 12p = \frac{135.69}{j\omega \cdot 12p \cdot 135.69 + 1} \quad (3.10)$$

$$Y = \frac{2.2M}{j\omega \cdot 12p \cdot 2.2M + 1} \quad (3.11)$$

The voltages across X and Y are:

$$V_x (\text{voltage on load}) = \frac{X}{X + Y} V_n \quad (3.12)$$

$$V_y (\text{voltage on openend}) = \frac{Y}{X + Y} V_n \quad (3.13)$$

The set up for near cable is shown in figure 14. Again, the simplified equations for the near cable are,

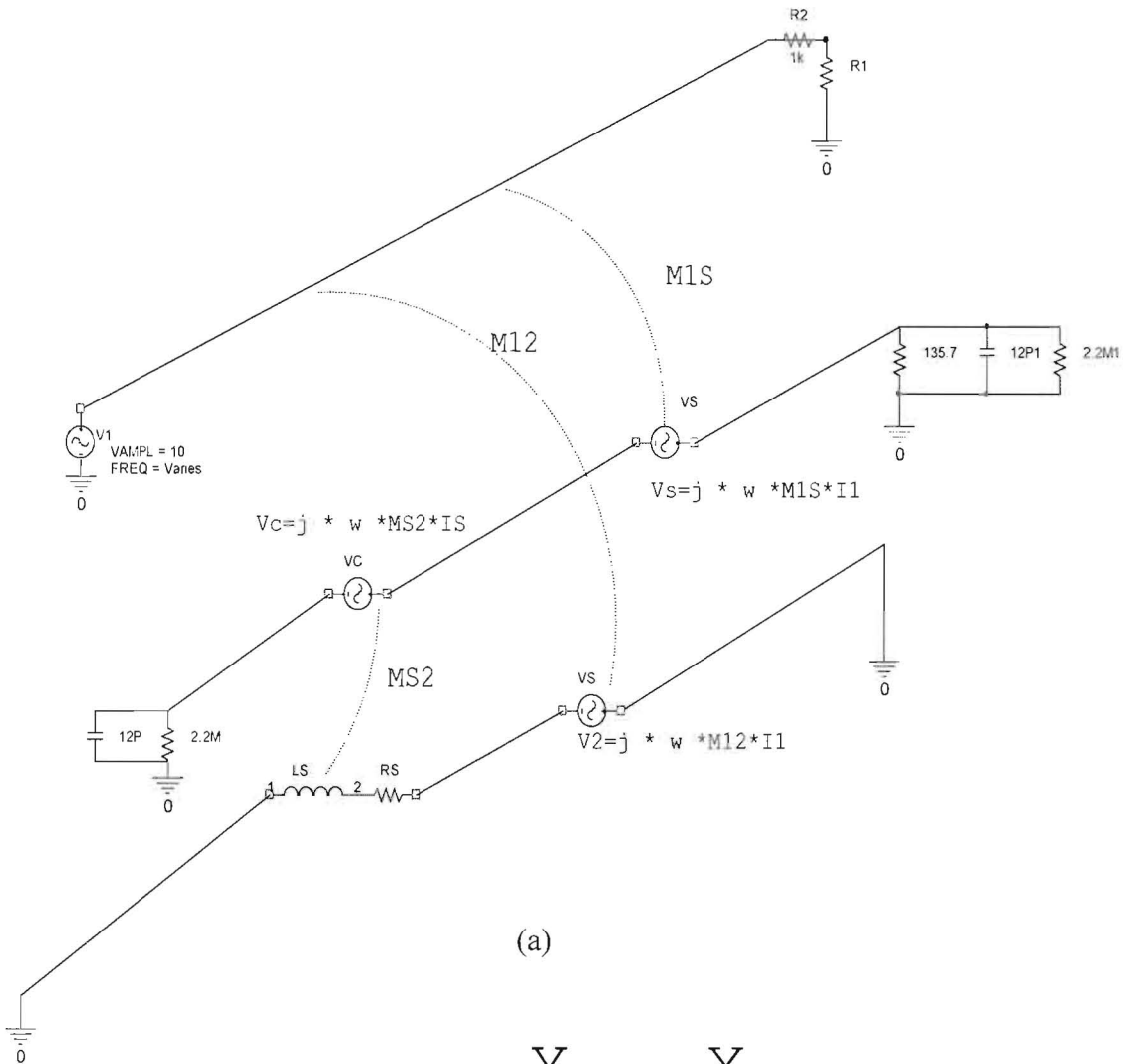
$$V_n = \frac{j\omega M_s (R_s + j\omega (M_s - M_{12})) V_1}{R_s + j\omega M_s} \frac{V_1}{R_1} \quad (3.14)$$

again, X is the total impedance at the right while y is the total impedance at the left as shown in figure 14 (equations 3.12, and 3.13),

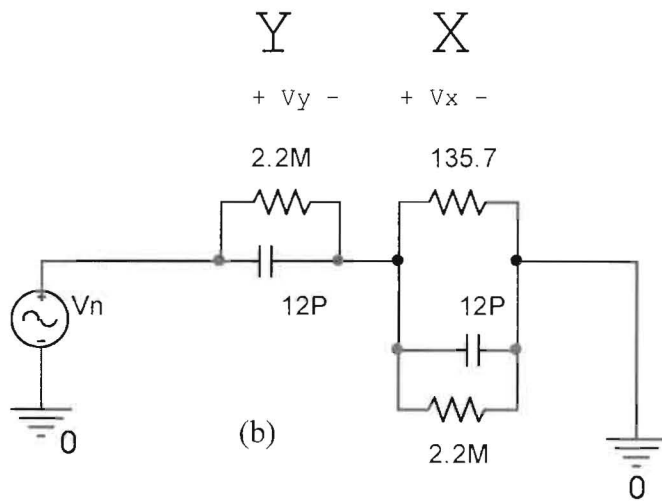
$$V_x (\text{voltage on load}) = \frac{X}{X + Y} V_n \quad (3.15)$$

$$V_y (\text{voltage on openend}) = \frac{Y}{X + Y} V_n \quad (3.16)$$

$R_s$  is the internal resistance for the wire which can be found through the calculation of the capacitive coupling or through measuring the  $R_{dc}$  (equations 2.2 and 2.4).



(a)



(b)

Figure 14: Inductive coupling between three wires, (a) the setup of near cable, (b) equivalent circuit.

# CHAPTER FOUR

## PER UNIT LENGTH PARAMETERS

The analysis of multi-data communication lines is somehow more difficult than the analysis of two transmission lines; however matrices provide an extension for many aspects from simple transmission-lines to multi-data communication lines [10].

To be able to predict the signal at the victim circuit, we need to go over the following three steps:

- The per unit length parameters should be determined.
- The equations for multi-transmission lines have to be solved.
- The terminal constraints that describe the edges at both side of multi-transmission lines should be substituted in the main equations to determine the unknown coefficients

Figure 15 shows examples of multi-transmission lines (MTL); normally these wires are surrounded by circular cylindrical dielectric insulations and assumed to be parallel to each other. The field structures surrounding the transmission line are assumed to be transverse electromagnetic (TEM).

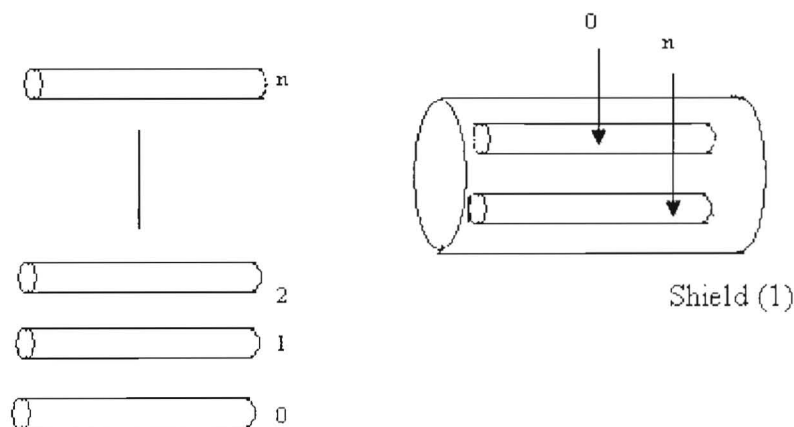


Figure 15: Examples of multi-transmission lines.

The MTL equations can be determined from per unit length parameters using circuit analysis as shown in figure 16:

$$\begin{aligned}
 -V_i(z,t) + V_i(z + \Delta z,t) &= -r_i \Delta z I_i(z,t) - r_o \Delta z \sum_{k=1}^n I_k(z,t) \\
 -l_{i1} \Delta z \frac{\partial I_1(z,t)}{\partial t} - l_{i2} \Delta z \frac{\partial I_2(z,t)}{\partial t} - \Lambda &- l_{ii} \Delta z \frac{\partial I_i(z,t)}{\partial t} - l_{in} \Delta z \frac{\partial I_n(z,t)}{\partial t}
 \end{aligned} \quad (4.1)$$

$$\begin{aligned}
 I_i(z + \Delta z,t) - I_i(z,t) &= -g_{i1} \Delta z (V_i - V_1) - \Lambda g_{ij} \Delta z (V_i - V_j) - \\
 \Lambda - g_{in} \Delta z (V_i - V_n) - c_{i1} \Delta z \frac{\partial (V_i - V_1)}{\partial t} - \Lambda &- c_{ii} \Delta z \frac{\partial V_i}{\partial t} - \Lambda \\
 - c_{in} \Delta z \frac{\partial (V_i - V_n)}{\partial t}
 \end{aligned} \quad (4.2)$$

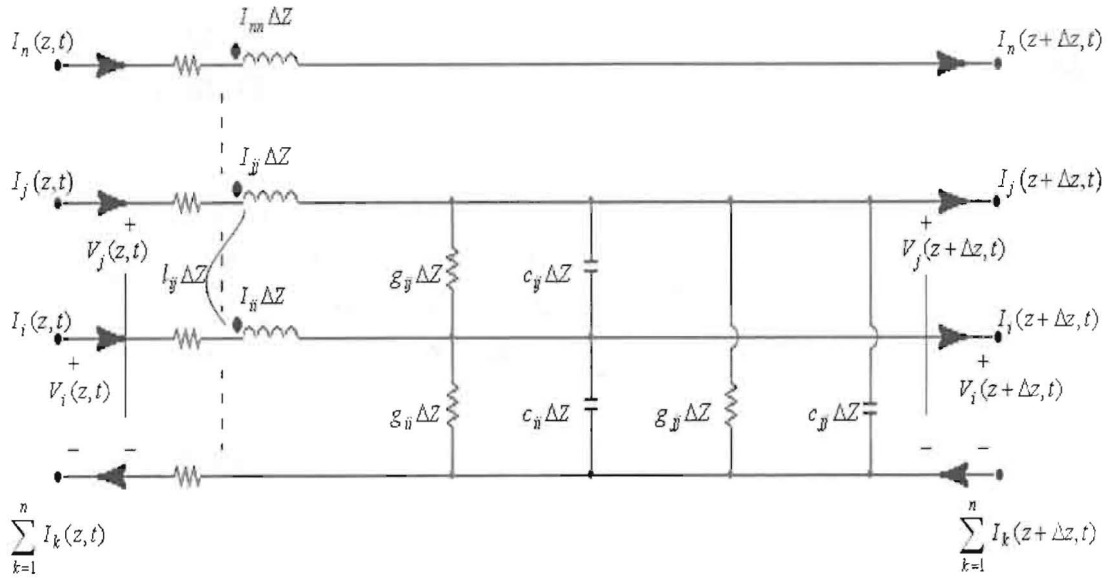


Figure 16: The per unit length parameters.

Dividing both sides of equations (4.1) and (4.2) by  $\Delta z$  and taking the limit  $\Delta z \rightarrow 0$ :

$$\frac{\partial}{\partial z} \bar{V}(z,t) = -R \bar{I}(z,t) - L \frac{\partial}{\partial z} \bar{I}(z,t) \quad (4.3)$$

$$\frac{\partial}{\partial z} \bar{I}(z,t) = -G \bar{V}(z,t) - C \frac{\partial}{\partial z} \bar{V}(z,t) \quad (4.4)$$

where:

$$\bar{V}(z,t) = \begin{bmatrix} V_1(z,t) \\ \text{M} \\ V_i(z,t) \\ \text{M} \\ V_n(z,t) \end{bmatrix} \quad (4.5a)$$

$$\bar{I}(z,t) = \begin{bmatrix} I_1(z,t) \\ \text{M} \\ I_i(z,t) \\ \text{M} \\ I_n(z,t) \end{bmatrix} \quad (4.5b)$$

$$\bar{L} = \begin{bmatrix} l_{11} & \Lambda & \Lambda & l_{1n} \\ \text{M} & \Lambda & \Lambda & \text{M} \\ \text{M} & \text{O} & \text{O} & \text{M} \\ l_{n1} & \text{O} & \text{O} & l_{nn} \end{bmatrix} \quad (4.6)$$

$$\bar{R} = \begin{bmatrix} (r_1 + r_o) & & r_o & r_o \\ \text{M} & (r_2 + r_o) & \text{O} & r_o \\ r_o & \text{O} & \text{O} & \text{M} \\ r_o & r_o & \text{K} & (r_n + r_o) \end{bmatrix} \quad (4.7)$$

$$\bar{G} = \begin{bmatrix} \sum_{k=1}^n g_{1k} & -g_{12} & \Lambda & -g_{1n} \\ -g_{21} & \sum_{k=1}^n g_{2k} & \Lambda & -g_{2n} \\ \text{M} & \text{O} & \text{O} & \text{M} \\ -g_{n1} & -g_{n2} & \Lambda & \sum_{k=1}^n g_{nk} \end{bmatrix} \quad (4.8)$$

$$\bar{C} = \begin{bmatrix} \sum_{k=1}^n c_{1k} & -c_{12} & \Lambda & -c_{1n} \\ -c_{21} & \sum_{k=1}^n c_{2k} & \Lambda & -c_{2n} \\ \text{M} & \text{O} & \text{O} & \text{M} \\ -c_{n1} & -c_{n2} & \Lambda & \sum_{k=1}^n c_{nk} \end{bmatrix} \quad (4.9)$$

If Multi- transmission lines are in a homogeneous medium characterized by permeability  $\mu$ , permittivity  $\varepsilon$ , and conductivity  $\sigma$ , the per unit length parameters are related by [12]:

$$\begin{aligned}\varepsilon\mu 1_n &= \overline{LC} = \overline{C}\overline{L} \\ \sigma\mu 1_n &= \overline{LG} = \overline{G}\overline{L}\end{aligned}\quad (4.10)$$

where:  $1_n$  is the identity matrix

The per unit length parameters are symmetric and positive definite matrixes. Doing some equation reductions and designating the capacitance matrix surrounded by free space, permeability  $\mu_o$ , permittivity  $\varepsilon_o$  as  $\overline{C}_o$ , the inductance matrix  $\overline{L}$  is obtained from  $\overline{C}_o$  as: [13]

$$\varepsilon_o\mu_o \overline{C}_o^{-1} = \overline{L} \quad (4.11)$$

We explain three methods for determining the per unit length parameters.

#### 4.1 Method 1: Matrix Definition

The inductance matrix is defined by,

$$\overline{\Psi} = \overline{L}\overline{I} \quad (4.12)$$

where  $\overline{L}$  matrix was defined in equation (4.6),  $\overline{I}$  matrix in equation (4.5), and  $\overline{\Psi}$  is a  $n \times 1$  matrix containing the total magnetic flux per unit length,  $\Psi_i$  penetrating the  $i$ -th circuit which is defined between the  $i$ -th line and the reference line [12]:

$$\overline{\Psi} = \begin{bmatrix} \Psi_1 \\ M \\ \Psi_i \\ M \\ \Psi_n \end{bmatrix} \quad (4.13)$$

This leads to the following relations:

$$l_{ii} = \frac{\Psi_i}{I_i} \Bigg|_{I_1=\Lambda = I_{i-1}=I_{i+1}=\Lambda = I_n=0} \quad (4.14a)$$

$$l_{ij} = \frac{\Psi_i}{I_j} \Bigg|_{I_1=\Lambda = I_{j-1}=I_{j+1}=\Lambda = I_n=0} \quad (4.14b)$$

We calculate the entries in L matrix by placing a current on one line, setting the currents on all other lines to zero, and determine the magnetic flux penetrating the other circuits.

Now, the capacitance matrix is defined by

$$\bar{Q} = \bar{C} \bar{V} \quad (4.15)$$

where  $\bar{C}$  matrix was defined in equation (4.9),  $\bar{V}$  matrix in equation (4.5), and  $\bar{Q}$  is a  $n \times 1$  matrix containing the total charge per unit length on the i-th conductor as  $q_i$  [12],

$$\bar{Q} = \begin{bmatrix} q_1 \\ M \\ q_i \\ M \\ q_n \end{bmatrix} \quad (4.16)$$

To obtain the entries on matrix  $\bar{C}$ , we need to have it in the following form:

$$\bar{V} = \bar{P} \bar{Q} \quad (4.17a)$$

$$\bar{C} = \bar{P}^{-1} \quad (4.17b)$$

This leads us to the following relations:

$$\bar{p}_{ii} = \frac{V_i}{q_i} \Big|_{q_1=\Lambda = q_{i-1} = q_{i+1} = \Lambda = q_n = 0} \quad (4.18a)$$

$$\bar{p}_{ij} = \frac{V_i}{q_j} \Big|_{q_1=\Lambda = q_{j-1} = q_{j+1} = \Lambda = q_n = 0} \quad (4.18b)$$

We calculate the entries in  $\bar{P}$  matrix by placing a charge  $q_i$  on one line, setting the charges on all other lines to zero, and determine the resulting voltage with respect to the reference line. Once the  $\bar{P}$  matrix is obtained,  $\bar{C}$  matrix is found using equation (4.17).

The conductance matrix is defined by,

$$\bar{I}_x = \bar{G} \bar{V} \quad (4.19)$$

where  $\bar{I}_x$  is a  $n \times 1$  matrix containing the total transverse conduction current passing between conductors per unit length, to all the line voltages producing it,  $\bar{G}$  matrix was defined in equation (4.8), and  $\bar{V}$  matrix in (4.5).



$$\bar{I}_x = \begin{bmatrix} I_{x1} \\ M \\ I_{xi} \\ M \\ I_{xn} \end{bmatrix} \quad (4.20)$$

This leads us to the following relations:

$$g_{ij} = \frac{I_{xi}}{V_j} \Big|_{V_1=\Lambda=V_{j-1}=V_{j+1}=\Lambda=V_n=0} \quad (4.21)$$

again, if the medium is homogeneous in  $\sigma$ ,  $\varepsilon$ , and  $\mu$ , we obtain the  $\bar{L}$ ,  $\bar{C}$ , and  $\bar{G}$  matrices by using one of the following equations as:

$$\bar{C} = \varepsilon\mu \bar{L}^{-1} \quad (4.22a)$$

$$\bar{L} = \varepsilon\mu \bar{C}^{-1} \quad (4.22b)$$

$$\bar{G} = \sigma\mu \bar{L}^{-1} = \frac{\sigma}{\varepsilon} \bar{C} \quad (4.22c)$$

## 4.2 Method 2: Wide Separation Approximations

Before we go further through this method, we need to discuss two concepts: magnetic flux per unit length, and voltage across two points. If we assume a current  $I$  is uniformly distributed over its area (circular cross section), the transverse magnetic field intensity  $\xi$  can be found using ampere's law and Biot-Savart law at distance  $r$  as:

$$\oint_c \xi \cdot d\vec{l} = I \quad (4.23a)$$

$$\xi = \frac{I}{2\pi r} \quad (4.23b)$$

Therefore the magnetic field is directly proportional to the current and inverse proportional to distance. Now, we need to find the magnetic flux from current through surface  $s$  as shown in figure 17 [15],

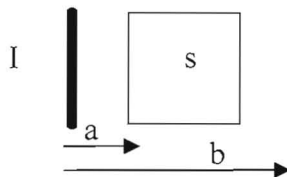


Figure 17: Magnetic flux per unit length of a wire.

$$\Psi = \Delta z \int_a^b \frac{\mu I}{2\pi r} dr \quad (4.24a)$$

$$\Psi = \Delta z \frac{\mu I}{2\pi} \ln\left(\frac{b}{a}\right) \quad (4.24b)$$

The magnetic flux per unit length is:

$$\frac{\Psi}{\Delta z} = \frac{\mu I}{2\pi} \ln\left(\frac{b}{a}\right) \quad (4.24c)$$

Next, voltage across two points is explained. Assume a line which is carrying a per unit length charge distribution of  $q$  is uniformly distributed as shown in figure 18, the electric field at distance  $r$  is obtained by using Gauss's law as:

$$\oint \epsilon E \cdot ds = Q \quad (4.25a)$$

$$E = \frac{q}{2\pi\epsilon r} \quad (4.25b)$$

The voltage between two points (a, b) as shown in figure 18.b.

$$V_{ba} = - \int_a^b \frac{q}{2\pi\epsilon r} dr = \frac{q}{2\pi\epsilon} \ln(a/b) \quad (4.26)$$

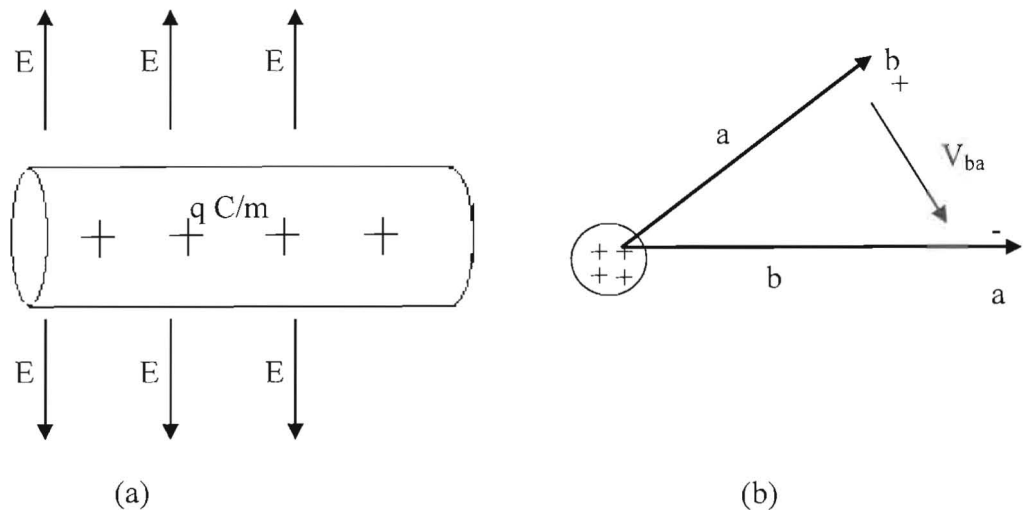


Figure 18: Charge distribution, (a) unit length distribution, (b) voltage between two points.

Let us consider the case for two wires of radius  $r_1, r_2$  as shown in figure 19,

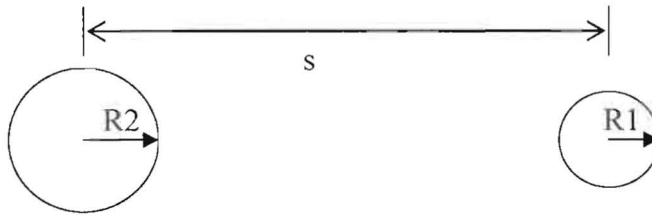


Figure 19: Two wires with  $s$  as separation.

The total flux per unit length between the two wires can be obtained with reference to equation 4.24 as:

$$\Psi = \frac{\mu I}{2\pi} \ln \left[ \frac{(s - r_2)(s - r_1)}{r_2 r_1} \right] \quad (4.27)$$

Substituting equation (4.12) in (4.27) gives the inductance  $l$  as:

$$l \cong \frac{\mu}{2\pi} \ln \left[ \frac{s^2}{r_2 r_1} \right] \quad (4.28)$$

The same procedure is used to find  $C$ . The voltage between the two lines can be obtained using equation (4.26):

$$V \cong \frac{q}{2\pi\epsilon} \ln \left[ \frac{s^2}{r_2 r_1} \right] \quad (4.29)$$

Substituting equation (4.15) in (4.29) results:

$$c = \frac{2\pi\epsilon}{\ln \left[ \frac{s^2}{r_2 r_1} \right]} \quad (4.30)$$

It has been assumed in Equations 4.30 and 4.28 that the lines are **widely separated**.

Finally, let us consider the case of  $(n+1)$  wires with the same radius in a homogeneous medium as shown in figure 20. With reference to equations 4.28 and 4.30, the entries in inductance matrix can be found as follows:

$$l_{ii} = \frac{\Psi_i}{I_i} \Big|_{I_1=\Lambda=I_{i-1}=I_{i+1}=\Lambda=I_n=0} \quad (4.31a)$$

$$l_{ii} = \frac{\mu}{2\pi} \ln \left[ \frac{s^2}{r_2 r_1} \right] = \frac{\mu}{2\pi} \ln \left[ \frac{d_{io}^2}{r^2} \right] = \frac{\mu}{\pi} \ln \left[ \frac{d_{io}}{r} \right] \quad (4.31b)$$

$$l_{ij} = \frac{\Psi_i}{I_j} \Big|_{I_1=\Lambda=I_{j-1}=I_{j+1}=\Lambda=I_n=0} \quad (4.32a)$$

$$l_{ij} = \frac{\mu}{2\pi} \ln \left[ \frac{s^2}{r_2 r_1} \right] = \frac{\mu}{2\pi} \ln \left[ \frac{d_{io} d_{jo}}{d_{ij} r} \right] \quad (4.32b)$$

Once the  $\bar{L}$  matrix has been found, the remaining matrices are found using one of the following equations [14],

$$\bar{C} = \varepsilon \mu \bar{L}^{-1} \quad (4.33a)$$

$$\bar{G} = \sigma \mu \bar{L}^{-1} = \frac{\sigma}{\varepsilon} \bar{C} \quad (4.33b)$$

or we find  $\bar{C}$  matrix using (4.30), and after that we can determine  $\bar{G}$  and  $\bar{L}$  matrices.

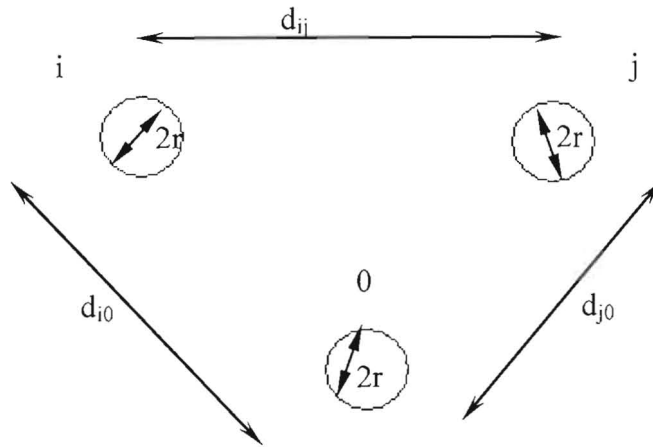


Figure 20: Three wires configuration.

### 4.3 Method 3: Numerical Methods

Numerical methods are needed since we can not derive an exact expression for more than two lines or wires with dielectric insulations. One of the important methods is Method of Moments (MOM) [9].

MOM depends on breaking each element into smaller areas, and assumes the distribution of a unit over these sub areas but with unknown amplitudes as shown in figure 26. In our situation the charge distribution will be non-uniform over the wire (in cases of near wires separation), so to model this we break each wire in to small area  $\Delta s$  and assume the distribution over these sub areas with unknown magnitudes, the charge over each sub area is  $\alpha_i$  , and the total charge on each wire is :

$$Q \cong \sum_{j=1}^N \alpha_j \Delta s_j \quad (4.34)$$

where N is the number of sub areas.

The main idea with this method is to determine the total voltage of each sub area as the sum of the contributions from the charges on each sub area.

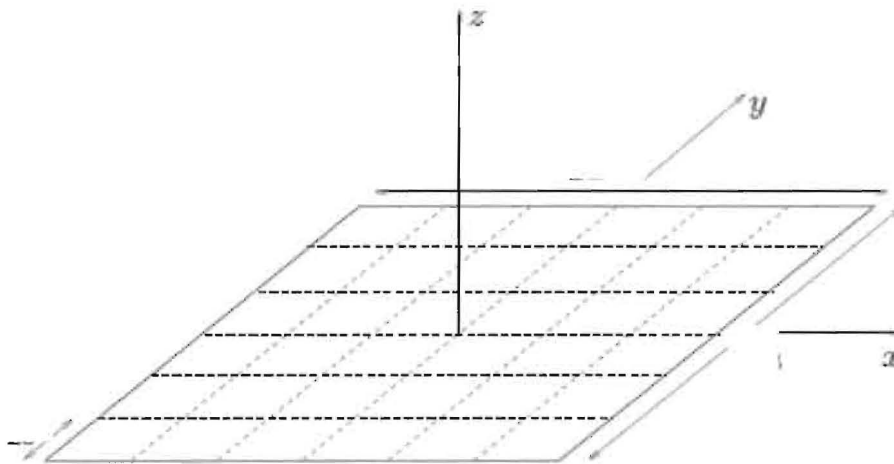


Figure 21: Method of Moments.

The total voltages on each sub areas are:

$$V_j = K_{j1}\alpha_1 + \dots + K_{j2N}\alpha_{2N} \quad (4.35)$$

It has been shown that [13]:

$$K_{ji} = \frac{V_j}{\alpha_i} = \frac{\Delta s_i}{4\pi\epsilon R_{ij}} \quad (4.36)$$

$$K_{ii} = \frac{\Delta w}{\pi\epsilon} \ln(1 + \sqrt{2}) = .8814 \frac{\Delta w}{\pi\epsilon} \quad (4.36)$$

$$C = \frac{Q}{2V} \quad (4.37)$$

where  $R_{ij}$  is the distance between the sub areas bearing the unknown charge and each sub area is  $\Delta w \times \Delta w$ . Using equation 4.37, the MOM matrix is:

$$\begin{bmatrix} K_{11} & \Lambda & K_{1(2N)} \\ M & O & M \\ K_{N1} & O & K_{(N)(2N)} \\ M & O & M \\ K_{(2N)1} & \Lambda & K_{(2N)(2N)} \end{bmatrix} \begin{bmatrix} \alpha_1 \\ M \\ \alpha_N \\ M \\ \alpha_{2N} \end{bmatrix} = \begin{bmatrix} +V \\ M \\ +V \\ -V \\ M \\ -V \end{bmatrix} = \begin{bmatrix} +1 \\ M \\ +1 \\ -1 \\ M \\ -1 \end{bmatrix} \quad (4.38)$$

Once the above matrix solved for  $\alpha_i$ , the total charge is determined from (4.34) and the total capacitance is determined from (4.37). The inductance and conductance matrices are determined from the capacitance matrix. In the following two chapters (5, 6), this method will be explained by an example.

# CHAPTER FIVE

## MATHEMATICAL MODEL

In order to say that a design has been considered as a model, the theoretical predictions should meet quite enough the practical or experimental measurements – under specific circumstances, variables, and assumptions [14].

Before we go further in this chapter, we need to distinguish between antenna coupling and cabling interference; actually they are under the same concepts and main equations, but cabling coupling refers to the unintended electromagnetic coupling between wires that are **in close** proximity. In other words, it's under **near** field coupling [3]. In this chapter we present a model that will predict the interference with adjacent cables. The objective here is to predict the interferences on both sides of an adjacent circuit.

### 5.1 General n Wires Equations:

The multi-conductor equations have been derived in the previous chapter (equations 4.3 and 4.4) as:

$$\frac{\partial}{\partial z} \bar{V}(z, t) = -\bar{R}\bar{I}(z, t) - \bar{L} \frac{\partial}{\partial z} \bar{I}(z, t) \quad (5.1)$$

$$\frac{\partial}{\partial z} \bar{I}(z, t) = -\bar{G}\bar{V}(z, t) - \bar{C} \frac{\partial}{\partial z} \bar{V}(z, t) \quad (5.2)$$

Since we are dealing with sinusoidal sources, the frequency responses in phasor forms are:

$$\frac{\partial}{\partial z} \hat{V}(z) = -\hat{Z} \hat{I}(z) \quad (5.3)$$

$$\frac{\partial}{\partial z} \hat{I}(z) = -\hat{Y} \hat{V}(z) \quad (5.4)$$

where:

$$\hat{Z} = \bar{R} + j\omega\bar{L} \quad (5.5a)$$

$$\hat{Y} = \bar{G} + j\omega\bar{C} \quad (5.5b)$$

$$\hat{V}_i = V_i(z) \angle \phi_i(z) \quad (5.6)$$

$$\hat{I}_i = I_i(z) \angle \phi_i(z) \quad (5.7)$$

Equations 5.3 and 5.4 are combined and written as:

$$\frac{\partial}{\partial z} \hat{X}(z) = \hat{A} \hat{X}(z) \quad (5.8)$$

where

$$\hat{X}(z) = \begin{bmatrix} \hat{V}(z) \\ \hat{I}(z) \end{bmatrix} \quad (5.9)$$

$$\hat{A} = \begin{bmatrix} 0 & -\hat{Z} \\ -\hat{Y} & 0 \end{bmatrix} \quad (5.10)$$

The main challenge in this chapter is to solve equation (5.9), and incorporate the terminal equations as a solution of the three steps that have been mentioned in the beginning of chapter three.

Consider n coupled, ordinary differential equation in **state variable** form as [13]:

$$\frac{\partial}{\partial t} X(t) = AX(t) + BU(t) \quad (5.11)$$

where:

$$X(t) = \begin{bmatrix} x_1(t) \\ \text{M} \\ x_i(t) \\ \text{M} \\ x_n(t) \end{bmatrix} \quad (5.12a)$$

$$U(t) = \begin{bmatrix} u_1(t) \\ \text{M} \\ u_i(t) \\ \text{M} \\ u_n(t) \end{bmatrix} \quad (5.12b)$$



$$A = \begin{bmatrix} a_{11} & \Lambda & a_{1n} \\ \text{M} & \text{O} & \text{M} \\ a_{n1} & \Lambda & a_{nn} \end{bmatrix} \quad (5.13a)$$

$$B = \begin{bmatrix} b_{11} & \Lambda & b_{1p} \\ \text{M} & \text{O} & \text{M} \\ b_{n1} & \Lambda & b_{np} \end{bmatrix} \quad (5.13b)$$

It has been shown that the solution of **state variable in (5.11)** is written as:

$$X(t) = \Phi(t - t_0)X(t_0) + \int_{t_0}^t \Phi(t - \tau)BU(\tau)d\tau \quad (5.14)$$

where:  $\Phi(t) = e^{At} = I_n + \frac{t_1}{1!}A_1 + \frac{t_2}{2!}A_2 + \Lambda$  (5.15)

Since equation (5.8) is similar to state variable equation (5.11) with  $U(t) = 0$ , the general solution of (5.8) is:

$$\begin{bmatrix} \hat{V}(z_2) \\ \hat{I}(z_2) \end{bmatrix} = \begin{bmatrix} \hat{\Phi}_{11}(z_2 - z_1) & \hat{\Phi}_{12}(z_2 - z_1) \\ \hat{\Phi}_{21}(z_2 - z_1) & \hat{\Phi}_{22}(z_2 - z_1) \end{bmatrix} \begin{bmatrix} \hat{V}(z_1) \\ \hat{I}(z_1) \end{bmatrix} \quad (5.16)$$

Substituting  $z_2 = \lambda$  and  $z_1 = 0$  in the previous equation gives:

$$\begin{bmatrix} \hat{V}(\lambda) \\ \hat{I}(\lambda) \end{bmatrix} = \begin{bmatrix} \hat{\Phi}_{11}(\lambda) & \hat{\Phi}_{12}(\lambda) \\ \hat{\Phi}_{21}(\lambda) & \hat{\Phi}_{22}(\lambda) \end{bmatrix} \begin{bmatrix} \hat{V}(0) \\ \hat{I}(0) \end{bmatrix} \quad (5.17)$$

The next four sub-sections describe four methods to obtain the  $\hat{\Phi}(\lambda)$  matrix.

### 5.1.1 Method 1: Definition

The simple way to obtain  $\hat{\Phi}(\lambda)$  matrix is by using (5.15) as:

$$\hat{\Phi}_{11}(\lambda) = 1_n + \frac{\lambda^2}{2!}\hat{Z}\hat{Y} + \frac{\lambda^4}{4!}[\hat{Z}\hat{Y}]^2 + \Lambda \quad (5.18)$$

$$\hat{\Phi}_{12}(\lambda) = -\frac{\lambda}{1!}\hat{Z} - \frac{\lambda^3}{3!}[\hat{Z}\hat{Y}]\hat{Z} - \frac{\lambda^5}{5!}[\hat{Z}\hat{Y}]^2\hat{Z} + \Lambda \quad (5.19)$$

$$\hat{\Phi}_{21}(\lambda) = -\frac{\lambda}{1!}\hat{Y} - \frac{\lambda^3}{3!}[\hat{Y}\hat{Z}]\hat{Y} - \frac{\lambda^5}{5!}[\hat{Y}\hat{Z}]^2\hat{Y} + \Lambda \quad (5.20)$$

$$\hat{\Phi}_{22}(\lambda) = 1_n + \frac{\lambda^2}{2!}\hat{Y}\hat{Z} + \frac{\lambda^4}{4!}[\hat{Y}\hat{Z}]^2 + \Lambda \quad (5.21)$$

### 5.1.2 Method 2: Similarity Transformation

The similarity transformation of currents and voltages are written as:

$$\hat{V}(z) = \hat{T}_V \hat{V}_M(z) \quad (5.22)$$

$$\hat{I}(z) = \hat{T}_I \hat{I}_M(z) \quad (5.23)$$

Substituting these into equation (5.8) gives:

$$\frac{\partial}{\partial z} \begin{bmatrix} \hat{V}_M \\ \hat{I}_M \end{bmatrix} = \begin{bmatrix} 0 & -\hat{T}_V^{-1} \hat{Z} \hat{T}_I \\ -\hat{T}_I^{-1} \hat{Y} \hat{T}_V & 0 \end{bmatrix} \begin{bmatrix} \hat{V}_M \\ \hat{I}_M \end{bmatrix} \quad (5.24)$$

where the main purpose of similarity transformation is to diagonalize the impedance matrix and admittance matrix, so equation (5.17) is much easier to solve since:

$$-\hat{T}_V^{-1} \hat{Z} \hat{T}_I = \begin{bmatrix} -\hat{z}_1 & 0 & 0 \\ 0 & 0 & 0 \\ 0 & 0 & -\hat{z}_n \end{bmatrix} \quad (5.25)$$

$$-\hat{T}_I^{-1} \hat{Y} \hat{T}_V = \begin{bmatrix} -\hat{y}_1 & 0 & 0 \\ 0 & 0 & 0 \\ 0 & 0 & -\hat{y}_n \end{bmatrix} \quad (5.26)$$

The general solution (5.24) is:

$$\hat{I}_M(z) = e^{-\hat{\gamma}z} \hat{I}_M^+ - e^{\hat{\gamma}z} \hat{I}_M^- \quad (5.27)$$

$$\hat{V}_M(z) = e^{-\hat{\gamma}z} \hat{V}_M^+ - e^{\hat{\gamma}z} \hat{V}_M^- \quad (5.28)$$

where:

$$\hat{I}_M^\pm = \begin{bmatrix} \hat{I}_{M1}^\pm \\ \mathbf{M} \\ \hat{I}_{M2}^\pm \end{bmatrix} \quad (5.29)$$

$$\hat{V}_M^\pm = \begin{bmatrix} \hat{V}_{M1}^\pm \\ \mathbf{M} \\ \hat{V}_{M2}^\pm \end{bmatrix} \quad (5.30)$$

$$\hat{T}_I' = \hat{T}_V^{-1} = \hat{T}' \quad (5.31)$$

$$\gamma^2 = \hat{T}'^{-1} \hat{Y} \hat{Z} \hat{T}' \quad (5.32)$$

The characteristic impedance matrix  $\hat{Z}_c$  equation becomes as:

$$\hat{Z}_c = \hat{Y}^{-1} \hat{T} \hat{\gamma} \hat{T}^{-1} \quad (5.33a)$$

$$\hat{Y}_c = \hat{Z}_c^{-1} \quad (5.33b)$$

Using the previous results, the actual voltages and currents are written as:

$$\hat{I}(z) = \hat{T} \left( e^{-\hat{\gamma}z} \hat{I}_M^+ - e^{\hat{\gamma}z} \hat{I}_M^- \right) \quad (5.34)$$

$$\hat{V}(z) = \hat{T}^{-1} \left( e^{-\hat{\gamma}z} \hat{V}_M^+ - e^{\hat{\gamma}z} \hat{V}_M^- \right) = \hat{Z}_c \hat{T} \left( e^{-\hat{\gamma}z} \hat{I}_M^+ - e^{\hat{\gamma}z} \hat{I}_M^- \right) \quad (5.35)$$

Evaluating equations 5.34 and 5.35 at  $z = 0$   $z = \lambda$ , and eliminating  $\hat{I}_M^\pm$  give the  $\Phi$  matrix as:

$$\hat{\Phi}_{11}(\lambda) = \frac{1}{2} \hat{Y}^{-1} \hat{T} \left( e^{\hat{\gamma}\lambda} + e^{-\hat{\gamma}\lambda} \right) \hat{T}^{-1} \hat{Y} \quad (5.35)$$

$$\hat{\Phi}_{12}(\lambda) = \frac{1}{2} \hat{Z}_c \left( \hat{T} \left( e^{\hat{\gamma}\lambda} - e^{-\hat{\gamma}\lambda} \right) \hat{T}^{-1} \right) \quad (5.36)$$

$$\hat{\Phi}_{21}(\lambda) = \frac{1}{2} \left( \hat{T} \left( e^{\hat{\gamma}\lambda} - e^{-\hat{\gamma}\lambda} \right) \hat{T}^{-1} \right) \hat{Y}_c \quad (5.37)$$

$$\hat{\Phi}_{22}(\lambda) = \frac{1}{2} \hat{T} \left( e^{\hat{\gamma}\lambda} + e^{-\hat{\gamma}\lambda} \right) \hat{T}^{-1} \quad (5.38)$$

### 5.1.3 Method 3: Hyperbolic Function

By defining the matrix exponentials and using equation 5.15 as:

$$e^{(\sqrt{\hat{Y}\hat{Z}})\lambda} = 1_n + \frac{\lambda}{1!} \sqrt{\hat{Z}\hat{Y}} + \frac{\lambda^2}{2!} [\sqrt{\hat{Z}\hat{Y}}]^2 + \Lambda \quad (5.39)$$

We define the matrix hyperbolic functions as:

$$\begin{aligned} \cosh(e^{(\sqrt{\hat{Y}\hat{Z}})\lambda}) &= \frac{1}{2} (e^{(\sqrt{\hat{Y}\hat{Z}})\lambda} + e^{-(\sqrt{\hat{Y}\hat{Z}})\lambda}) = \\ &= 1_n + \frac{\lambda^2}{2!} \left( \sqrt{\hat{Z}\hat{Y}} \right)^2 + \frac{\lambda^4}{4!} [\sqrt{\hat{Z}\hat{Y}}]^4 + \Lambda = \frac{1}{2} \hat{T} \left( e^{\hat{\gamma}\lambda} + e^{-\hat{\gamma}\lambda} \right) \hat{T}^{-1} \end{aligned} \quad (5.40)$$

$$\begin{aligned} \sinh(e^{(\sqrt{\hat{Y}\hat{Z}})\lambda}) &= \frac{1}{2} (e^{(\sqrt{\hat{Y}\hat{Z}})\lambda} - e^{-(\sqrt{\hat{Y}\hat{Z}})\lambda}) = \\ &= \frac{\lambda}{1!} \left( \sqrt{\hat{Z}\hat{Y}} \right) + \frac{\lambda^3}{3!} [\sqrt{\hat{Z}\hat{Y}}]^3 + \Lambda = \frac{1}{2} \hat{T} \left( e^{\hat{\gamma}\lambda} - e^{-\hat{\gamma}\lambda} \right) \hat{T}^{-1} \end{aligned} \quad (5.41)$$

In terms of these symbolic definitions, the  $\Phi$  matrix is written as;

$$\hat{\Phi}_{11}(\lambda) = \cosh(\sqrt{\hat{Z}\hat{Y}} \lambda) \quad (5.42)$$

$$\hat{\Phi}_{12}(\lambda) = -\hat{Z}_c \sinh(\sqrt{\hat{Y}\hat{Z}} \lambda) \quad (5.43)$$

$$\hat{\Phi}_{21}(\lambda) = -\hat{Z}_c^{-1} \sinh(\sqrt{\hat{Z}\hat{Y}} \lambda) \quad (5.44)$$

$$\hat{\Phi}_{22}(\lambda) = \cosh(\sqrt{\hat{Y}\hat{Z}} \lambda) \quad (5.45)$$

#### 5.1.4 Method 4: Ideal Case

In this section, three assumptions are made, in order to simplify calculations in the previous three sub sections as follows:

- 1- Perfect conductor: for this case  $R = 0$  , the product of impedance and admittance matrices is

$$\hat{Y}\hat{Z} = j\omega\overline{GL} - \omega^2\overline{CL} \quad (5.46)$$

- 2- Homogeneous surrounding medium: which satisfies the following property

$$\begin{aligned} \overline{C}\overline{L} &= \overline{L}\overline{C} = \mu\epsilon I_n \\ \overline{G}\overline{L} &= \overline{L}\overline{G} = \mu\sigma I_n \end{aligned} \quad (5.47)$$

- 3- Lossless surrounding medium: which means  $\sigma = 0$  which implies that the propagation constant  $\gamma$  becomes;

$$\gamma = j\omega\sqrt{\mu\epsilon} \quad (5.48)$$

$$\text{where: } v = \frac{1}{\sqrt{\mu\epsilon}} \quad (5.49a)$$

$$\beta = \omega\sqrt{\mu\epsilon} \quad (5.49b)$$

The  $\Phi$  parameter matrix becomes for the previous assumptions:

$$\hat{\Phi}_{11}(\lambda) = \cos(\beta\lambda)I_n \quad (5.50)$$

$$\hat{\Phi}_{12}(\lambda) = -j\sin(\beta\lambda)\hat{Z}_c \quad (5.51)$$

$$\hat{\Phi}_{21}(\lambda) = -j\sin(\beta\lambda)\hat{Z}_c^{-1} \quad (5.52)$$

$$\hat{\Phi}_{22}(\lambda) = \cos(\beta\lambda)I_n \quad (5.53)$$

## 5.2 The Terminal Constraints

The purpose of this section is to incorporate the terminal conditions into the main equations to explicitly determine the terminal voltages and currents and complete the last step. The constraint equations are provided by the terminal conditions at  $z = 0$  and at  $z = \lambda$ . The deriving sources and load impedances are contained in these terminal networks that are attached to the two ends of the lines. Figure 22 shows the terminal networks at  $z = 0$  and at  $z = \lambda$ .

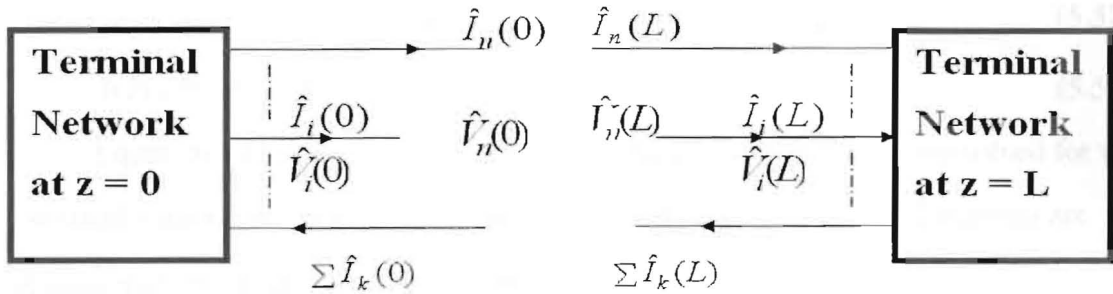


Figure 22: Terminal Networks.

The relationship is a linear combination of the port voltages and currents as [11]:

$$\hat{V}(0) = \hat{V}_s - \hat{Z}_s \hat{I}(0) \quad (5.54a)$$

$$\hat{V}(\lambda) = \hat{V}_L - \hat{Z}_L \hat{I}(\lambda) \quad (5.54b)$$

The  $n \times 1$  vectors  $\hat{V}_s$  and  $\hat{V}_L$  contain the effects of the independent voltages and current sources at  $z = 0$  and at  $z = \lambda$ , respectively. The  $n \times n$  matrices  $\hat{Z}_s$  and  $\hat{Z}_L$  contain the effects of impedances at  $z = 0$  and at  $z = \lambda$ , respectively.

$$\hat{V}_s = \begin{bmatrix} \hat{V}_{s1} \\ \mathbf{M} \\ \hat{V}_{sn} \end{bmatrix} \quad (5.55a)$$

$$\hat{V}_L = \begin{bmatrix} \hat{V}_{L1} \\ \mathbf{M} \\ \hat{V}_{Ln} \end{bmatrix} \quad (5.55b)$$

$$\hat{Z}_s = \begin{bmatrix} \hat{Z}_{s1} & 0 & 0 \\ 0 & 0 & 0 \\ 0 & 0 & \hat{Z}_{sn} \end{bmatrix} \quad (5.56a)$$

$$\hat{Z}_L = \begin{bmatrix} \hat{Z}_{L1} & 0 & 0 \\ 0 & 0 & 0 \\ 0 & 0 & \hat{Z}_{Ln} \end{bmatrix} \quad (5.56b)$$

A method for incorporating the terminal conditions is to substitute the terminal equations in (5.54) into the  $\Phi$  parameter matrix (5.17) to yield:

$$\left( \hat{\Phi}_{12} - \hat{\Phi}_{11} \hat{Z}_s - \hat{Z}_L \hat{\Phi}_{22} + \hat{Z}_L \hat{\Phi}_{21} \hat{Z}_s \right) \hat{I}(0) = \hat{V}_L - (\hat{\Phi}_{11} - \hat{Z}_L \hat{\Phi}_{21}) \hat{V}_s \quad (5.57)$$

$$\hat{I}(\lambda) = \hat{\Phi}_{21} \hat{V}_s + (\hat{\Phi}_{22} - \hat{\Phi}_{21} \hat{Z}_s) \hat{I}(0) \quad (5.58)$$

Equation 5.57 and 5.58 are a set of  $n$  algebraic equations which are solved for the  $n$  terminal currents at  $z = 0$ ,  $\hat{I}(0)$ . Once these are solved, the  $n$  terminal currents are obtained from (5.58) at  $z = \lambda$ ,  $\hat{I}(\lambda)$ . The  $n$  terminal voltages  $\hat{V}(0)$  and  $\hat{V}(\lambda)$  are obtained from the terminal equations in (5.54).

## CHAPTER SIX

### THREE RIP CORD CABLES

In this chapter we deal with three Rip Cord cables as a special case from the previous chapter with the following assumptions:

- The wires are symmetric and parallel.
- The wires and the surrounding medium are lossless.
- The medium is homogeneous.
- The source signals are sinusoids.

Rip Cord cables are a parallel cord of wires situated under PVC (Polyvinyl chloride) insulation [14]. The cross section area of Rip Cord was measured using a microscope; figure 23 shows the cross section of a Rip Cord of one and two cables. The dimensions were recorded in order to get wire radius, center to center separation, and dielectric thickness. The radius of the Rip Cord is around 18.11 mils. The insulation thickness of the Rip Cord is around 18.11 mils. The center to center distance is around 97.26 mils.

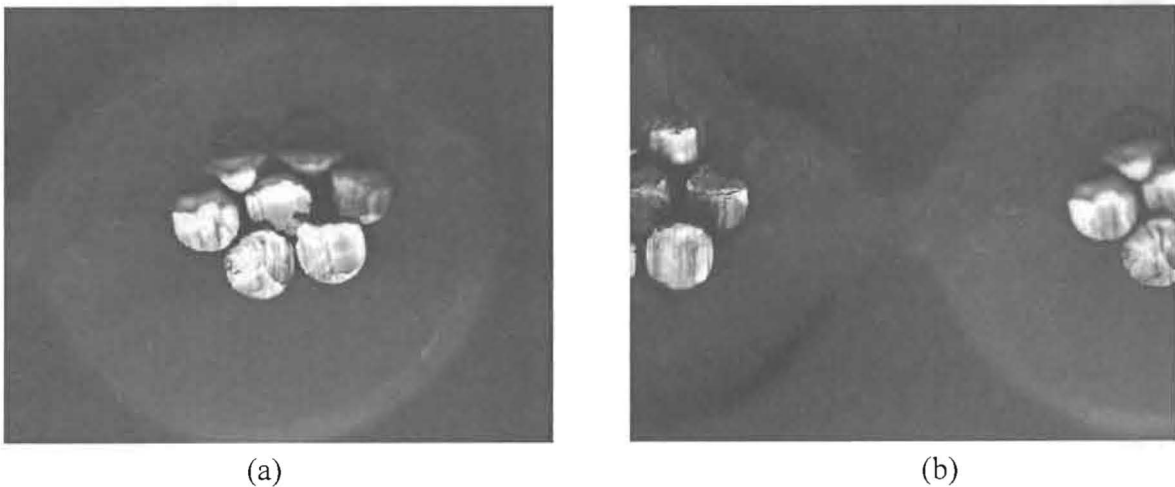


Figure 23: Cross section of Rip Cord wires, (a) one wire, (b) two wires.

The purpose of this chapter is to drive the mathematical model of three Rip Cords and to test if the model will predict the measurements or not. Figure 24 and figure 25 show three Rip Cords in a lossless homogenous medium characterized by permittivity  $\epsilon$  and permeability  $\mu$ .

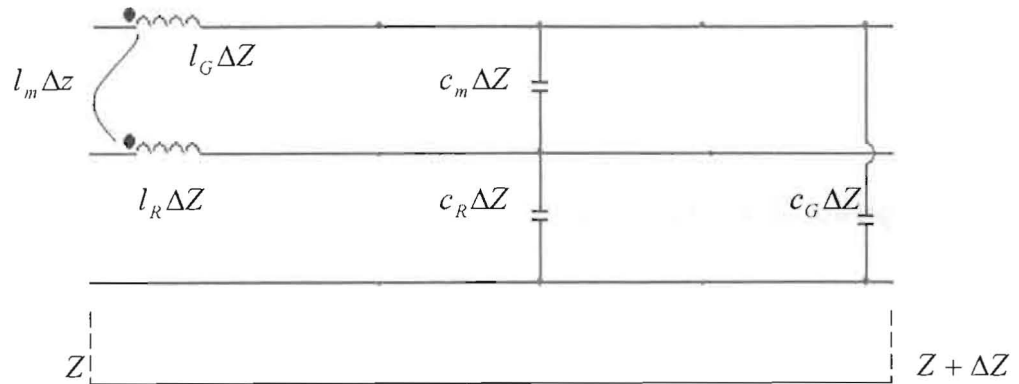


Figure 24: Parameters per unit length of three Rip Cords.

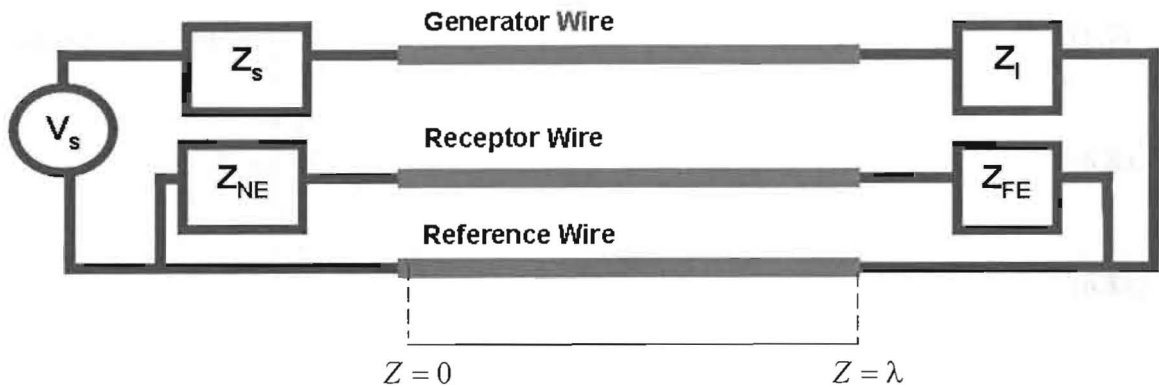


Figure 25: Three Rip Cords connection inside a circuit.

Since  $\bar{R}$  and  $\bar{G}$  matrices are equal to zero, The Multi-conductor equations become:

$$\frac{\partial}{\partial z} \hat{V}(z) = -\bar{L} \frac{\partial}{\partial z} \hat{I}(z) \quad (6.1)$$

$$\frac{\partial}{\partial z} \hat{I}(z) = -\bar{C} \frac{\partial}{\partial z} \hat{V}(z) \quad (6.2)$$



where: 
$$\hat{V}(z) = \begin{bmatrix} \hat{V}_G(z) \\ \hat{V}_R(z) \end{bmatrix} \quad (6.3a)$$

$$\hat{I}(z) = \begin{bmatrix} \hat{I}_G(z) \\ \hat{I}_R(z) \end{bmatrix} \quad (6.3a)$$

$$\bar{L} = \begin{bmatrix} l_G & l_M \\ l_M & l_R \end{bmatrix} \quad (6.4a)$$

$$\bar{C} = \begin{bmatrix} c_G + c_M & -c_M \\ -c_M & c_R + c_M \end{bmatrix} \quad (6.4b)$$

Because of the assumption of homogeneous surrounding medium, the following property is applied:

$$\bar{L}\bar{C} = \bar{C}\bar{L} = \varepsilon\mu l_2 = \frac{1}{v^2} l_2 \quad (6.5)$$

The terminal conditions are written as:

$$\hat{V}(0) = \hat{V}_s - \hat{Z}_s \hat{I}(0) \quad (6.6a)$$

$$\hat{V}(\lambda) = \hat{Z}_L \hat{I}(\lambda) \quad (6.6b)$$

where: 
$$\hat{V}_s = \begin{bmatrix} \hat{V}_s \\ 0 \end{bmatrix} \quad (6.7)$$

$$\hat{Z}_s = \begin{bmatrix} \hat{Z}_s & 0 \\ 0 & \hat{Z}_{NE} \end{bmatrix} \quad (6.8a)$$

$$\hat{Z}_L = \begin{bmatrix} \hat{Z}_L & 0 \\ 0 & \hat{Z}_{FE} \end{bmatrix} \quad (6.8b)$$

The  $\Phi$  matrix becomes:

$$\begin{bmatrix} \hat{V}(\lambda) \\ \hat{I}(\lambda) \end{bmatrix} = \begin{bmatrix} \hat{\Phi}_{11}(\lambda) & \hat{\Phi}_{12}(\lambda) \\ \hat{\Phi}_{21}(\lambda) & \hat{\Phi}_{22}(\lambda) \end{bmatrix} \begin{bmatrix} \hat{V}(0) \\ \hat{I}(0) \end{bmatrix} \quad (6.9)$$

where: 
$$\hat{\Phi}_{11}(\lambda) = \cos(\beta\lambda)l_n = Cc l_2 \quad (6.10)$$

$$\hat{\Phi}_{12}(\lambda) = -j \sin(\beta\lambda) \hat{Z}_c = -j\omega\lambda S\bar{L} \quad (6.11)$$

$$\hat{\Phi}_{21}(\lambda) = -j \sin(\beta\lambda) \hat{Z}_c^{-1} = -j\omega\lambda S\bar{C} \quad (6.12)$$

$$\hat{\Phi}_{22}(\lambda) = \cos(\beta\lambda)l_n = Cc l_2 \quad (6.13)$$

$$Cc = \cos(\beta\lambda) \quad (6.14)$$

$$S = \cos(\beta\lambda)/(\beta\lambda) \quad (6.15)$$

$$v = \frac{1}{\sqrt{\epsilon\mu}} = \frac{\omega}{\beta}$$

$$(6.16)$$

Now, substituting the terminal equation into the  $\Phi$  matrix gives:

$$\left(-\hat{\Phi}_{12} + \hat{\Phi}_{11}\hat{Z}_S + \hat{Z}_L\hat{\Phi}_{22} - \hat{Z}_L\hat{\Phi}_{21}\hat{Z}_S\right)\hat{I}(0) = (\hat{\Phi}_{11} - \hat{Z}_L\hat{\Phi}_{21})\hat{V}_S \quad (6.17)$$

$$\left(-\hat{\Phi}_{12} + \hat{\Phi}_{11}\hat{Z}_S + \hat{Z}_S\hat{\Phi}_{22} - \hat{Z}_S\hat{\Phi}_{21}\hat{Z}_L\right)\hat{I}(\lambda) = \hat{V}_S \quad (6.18)$$

Solving these equations for  $\hat{I}_R(0)$  and  $\hat{I}_R(\lambda)$ , and substituting the results.  $\hat{V}_R(0)$  and  $\hat{V}_R(\lambda)$  become as:

$$\hat{V}_R(\lambda) = \frac{j\omega\lambda SZ_{FE}(c_M Z_L Z_{NE} - l_M)V_S}{\Delta} \quad (6.19)$$

$$\begin{aligned} \hat{V}_R(0) &= \frac{j\omega\lambda SZ_{NE}V_S}{\Delta} \times Cc(Z_{FE}Z_Lc_M + l_M) \\ &+ \frac{j\omega\lambda SZ_{NE}V_S}{\Delta} \times j\omega\lambda S(Z_{FE}c_M l_G + Z_L l_M(c_G + c_M)) \end{aligned} \quad (6.20)$$

$$\begin{aligned} \Delta &= (Z_S + Z_L)(Z_{NE}Z_{FE})C_c^2 \\ &- \omega^2\lambda^2 S^2 \left( \begin{array}{l} (Z_L Z_S(c_G + c_M) + l_G) \cdot \\ (Z_{NE}Z_{FE}(c_R + c_M) + l_R) \\ -(l_M - c_M Z_S Z_{FE})(l_M - c_M Z_L Z_{NE}) \end{array} \right) \\ &+ j\omega\lambda S C_c \left( \begin{array}{l} (Z_{NE} + Z_{FE})(Z_L Z_S(c_G + c_M) + l_G) \\ + (Z_S + Z_L)(Z_{NE}Z_{FE}(c_R + c_M) + l_R) \end{array} \right) \end{aligned} \quad (6.21)$$

Equations 6.19 to 6.21 are written simply as:

$$\hat{V}_R(\lambda) = \frac{j\omega S M_{FE} V_S}{\Delta} \quad (6.22)$$

$$\hat{V}_R(0) = \frac{S V_S}{\Delta} (j\omega M_{NE} Cc + (j\omega)^2 T K_{NE} S) \quad (6.23)$$

$$\Delta = C_c^2 + (j\omega)^2 S^2 \tau_G \tau_R P + j\omega C_c S (\tau_G + \tau_R) \quad (6.24)$$

where:

$$M_{NE} = M_{NE}^{IND} + M_{NE}^{CAP} \quad (6.25)$$

$$M_{FE} = M_{FE}^{IND} + M_{FE}^{CAP} \quad (6.26)$$

$$M_{NE}^{IND} = \frac{Z_{NE} l_M \lambda}{(R_{NE} + R_{FE})(R_S + R_L)} \quad (6.27)$$

$$M_{FE}^{IND} = \frac{Z_{FE} l_M \lambda}{(R_{NE} + R_{FE})(R_S + R_L)} \quad (6.28)$$

$$M_{NE}^{CAP} = M_{FE}^{CAP} = \frac{Z_L Z_{FE} Z_{NE} c_M \lambda}{(R_{NE} + R_{FE})(R_S + R_L)} \quad (6.29)$$

$$K_{NE} = M_{NE}^{IND} \frac{1}{\sqrt{1-K^2}} \alpha_{LG} + M_{NE}^{CAP} \frac{1}{\sqrt{1-K^2}} \alpha_{LG} \quad (6.30)$$

$$K = \frac{l_M}{\sqrt{l_G l_R}} \quad (6.31)$$

$$Z_{CG} = \nu l_G \sqrt{1-K^2} \quad (6.32)$$

$$Z_{CR} = \nu l_R \sqrt{1-K^2} \quad (6.33)$$

$$T = \frac{\lambda}{\nu} \quad (6.34)$$

$$\alpha_{SG} = Z_S / Z_{CG} \quad (6.35)$$

$$\alpha_{LG} = Z_L / Z_{CG} \quad (6.36)$$

$$\alpha_{SR} = Z_{NE} / Z_{CR} \quad (6.37)$$

$$\alpha_{LR} = Z_{FE} / Z_{CR} \quad (6.38)$$

$$P = \left[ 1 - K^2 \frac{(1 - \alpha_{SG} \alpha_{LR})(1 - \alpha_{LG} \alpha_{SR})}{(1 + \alpha_{SG} \alpha_{LG})(1 + \alpha_{SR} \alpha_{LR})} \right] \quad (6.39)$$

$$\tau_G = \frac{T}{\sqrt{1-K^2}} \left( \frac{1 + \alpha_{SG} \alpha_{LG}}{\alpha_{SG} \alpha_{LG}} \right) \quad (6.40)$$

$$\tau_R = \frac{T}{\sqrt{1-K^2}} \left( \frac{1 + \alpha_{SR} \alpha_{LR}}{\alpha_{SR} \alpha_{LR}} \right) \quad (6.41)$$

## 6.1 Experiment Setup

All the experiments were performed inside an electrically shielded enclosure, (i.e. the NoiseKen tent [17]) in order to reduce the amount of background noise being picked up by the experiment. Figure 26 is the tent with a PC (outside) used to collect the data (coupled noise) recorded by the VEE Pro which is an Agilent software and we used it to control Agilent devices remotely. Figure 27 shows the test setup, featuring the test fixture, Agilent function generator, Agilent mixed signal oscilloscope, and LeCroy scope.



Figure 26: NoiseKen tent.



Figure 27: Test setup.

The power cables and network connections were wrapped in a shroud of shielding material, the same as the tents composition and routed outside, connecting to the near by outlet and PC. Special care was taken in positioning the equipment, to achieve a minimum of ambient noises picked up and eliminate erroneous measurements. All the experiments were done with the tent closed, and the measurements were taken using

VEE Pro as shown in figure 28. The measurements were saved and exported to MATLAB for manipulating.

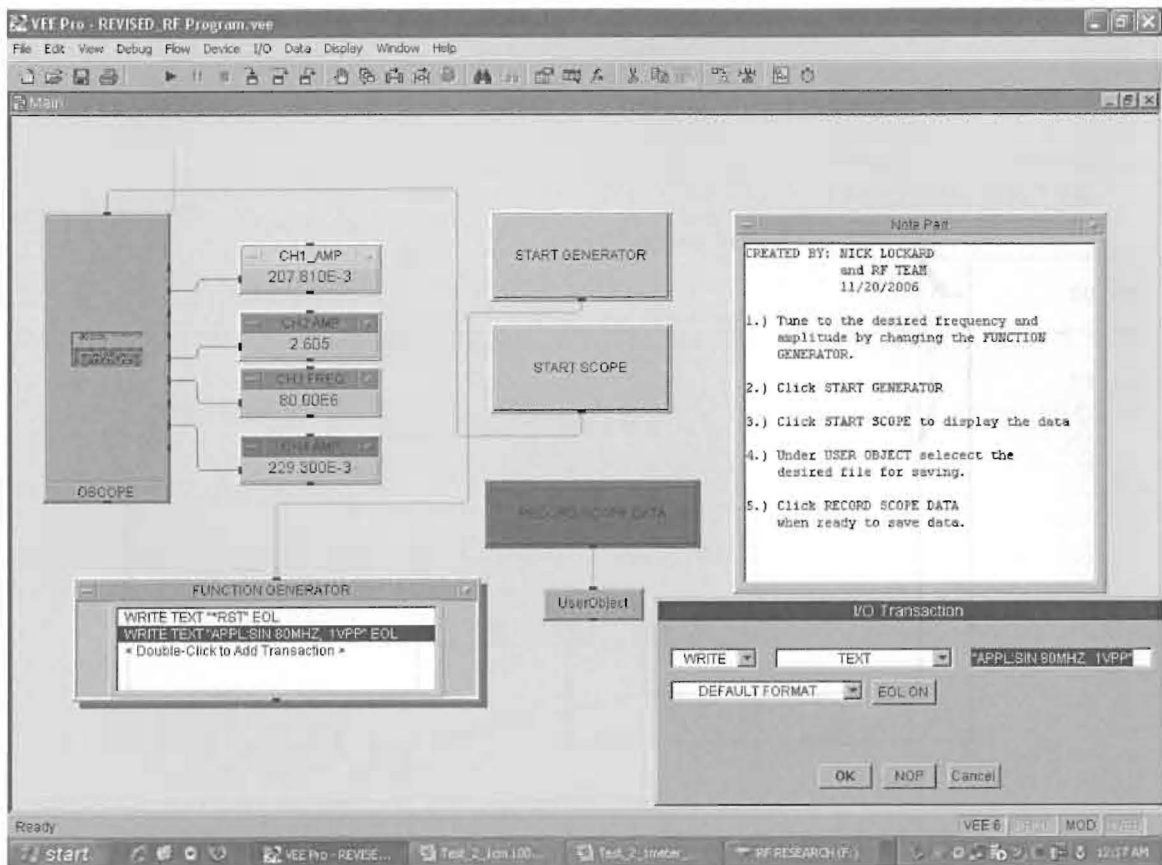


Figure 28: VEE Pro.

The Rip Cord length of 1.7 meters was chosen because it is typical in automotive applications. The test fixture (as shown in figure 27) was built to the length of 2 meters to easily accommodate the test samples that were 1.7 meter in length. The noise wire is bent at the ends to avoid the stray noise that may couple into the measurements probes. The experiment was strictly concerned with noise introduced on the test wire itself. Figure 29 and figure 30 show the basic measurement setup.

The noise characteristics of each wire were quantified by taking peak to peak voltage measurements at both ends of the wire. Three channels of the Agilent oscilloscope were utilized. All channels are set to 1 M $\Omega$  input impedance and DC coupling. The probes were set to 2.2M $\Omega$  parallel with 12 pF. Channel two is connected

to the noise source for comparison. Channel four is connected to the open end of the test sample wire. Channel one is connected to the 137.5  $\Omega$  termination. The probe leads attached to the oscilloscope are taped down to prevent movement during testing and insuring that leads are well spaced avoiding cross talk.

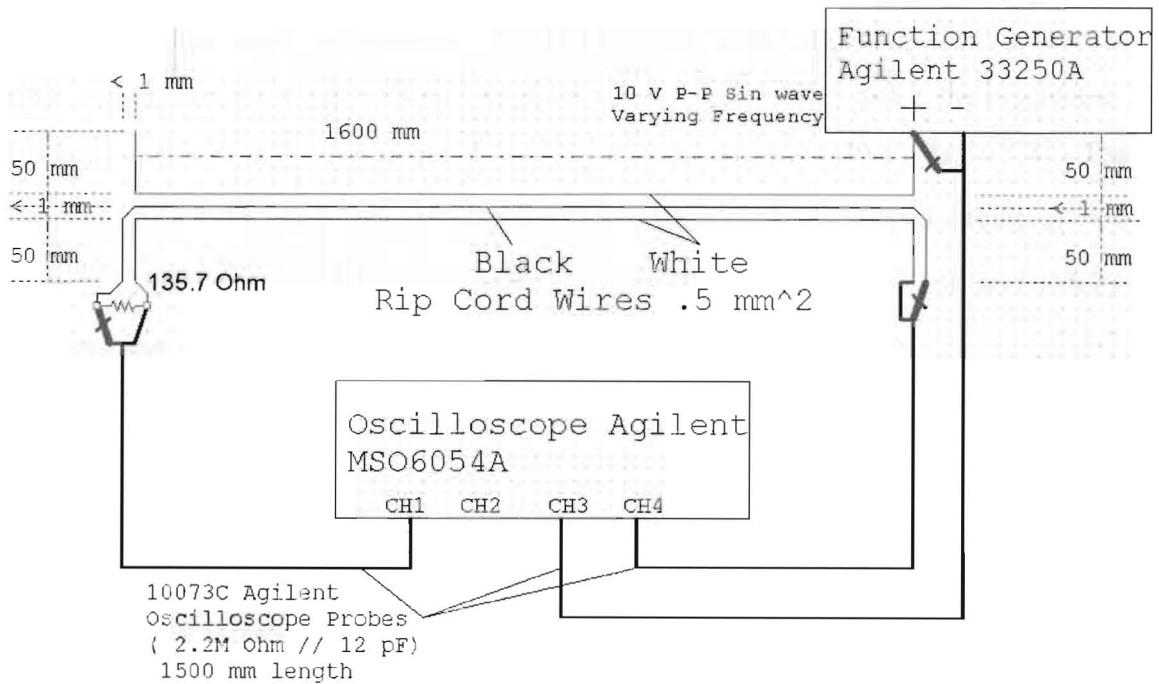


Figure 29: Physical representation of test setup.

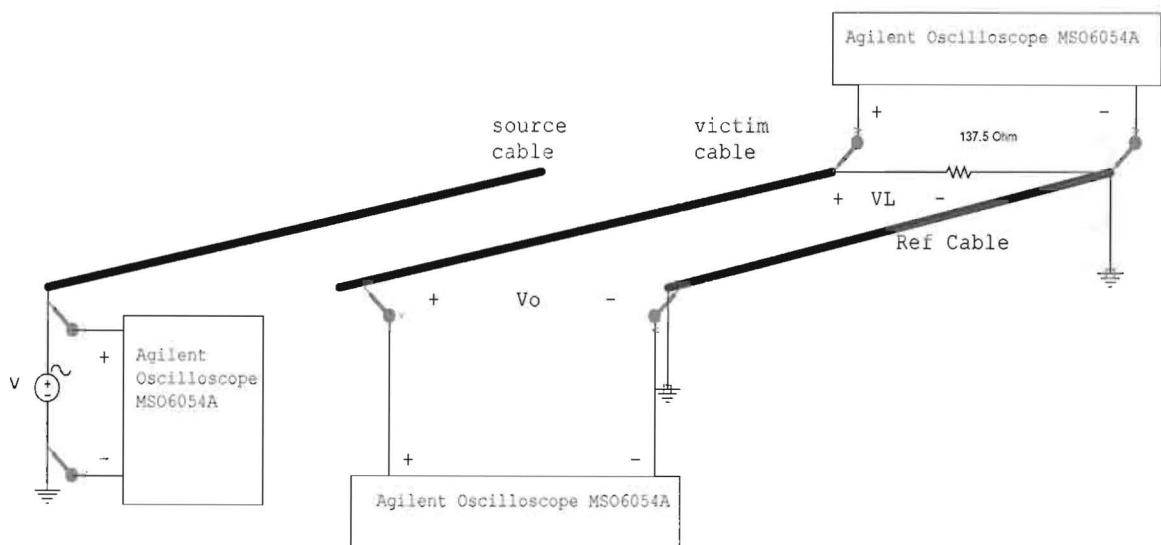


Figure 30: Three dimensions of test setup.

## 6.2 Model versus Measurements

In this section we show some computed and experimental results that demonstrate the prediction methods of this chapter. The prediction model is implemented in the computer program **Tamer.m** described in appendix A.

Three Rip Cords are tested as shown in figure 29 and figure 30. The setup consists of three Rip Cords of total length 1.7 m. The radius of the Rip Cord is 18.11 mils, the adjacent wire separation is 92.91 mils (i.e. 1 cm = 398.3 mils), the insulation thickness is 18.11 mils, and the insulation is polyvinyl Chloride (PVC) ( $\epsilon_r = 3.4$ ). The load impedances are as follows (with reference to figure 25):  $Z_l = \text{open circuit}$ ,  $Z_s = 0$ ,  $Z_{NE} = 2.2M\Omega$  parallel with 12 pF, and  $Z_{FE} = 2.2M\Omega$  parallel with 12 pF and 135.7  $\Omega$ . The terminal conditions or constrains are shown in figure 31, where:

$$\hat{V}_s = \begin{bmatrix} V_s \\ 0 \end{bmatrix} \quad (6.42)$$

$$\hat{Z}_s = \begin{bmatrix} 0 & 0 \\ 0 & \hat{Z}_{NE} \end{bmatrix} \quad (6.43)$$

$$\hat{Z}_L = \begin{bmatrix} \infty & 0 \\ 0 & \hat{Z}_{FE} \end{bmatrix} \quad (6.44)$$

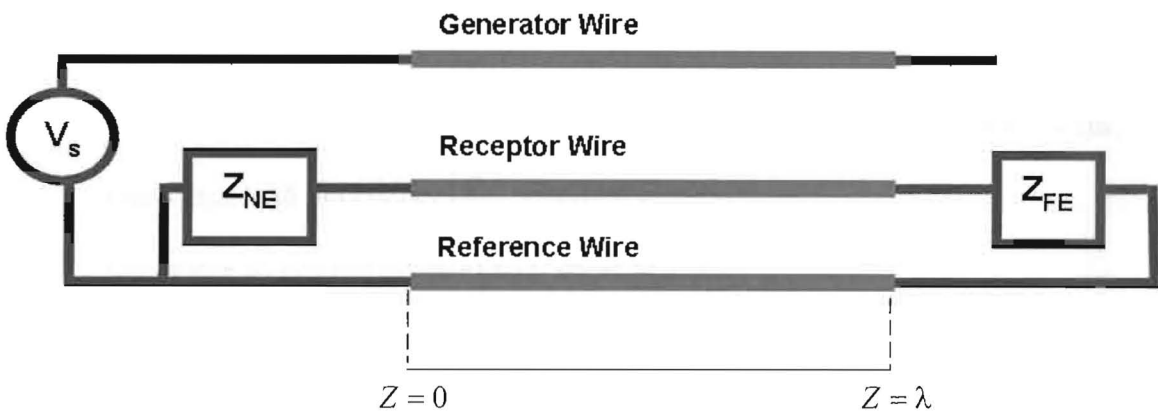


Figure 31: Three Rip Cords terminal conditions.

Five different configurations of three Rip Cords with nine different experimental samples are prepared, tested, and presented in the next sub sections as:

- Section 6.2.1 (basic configuration): This is shown in figure 31 with all previous discussions. Three samples are tested.
- Section 6.2.2 (changing voltage source noise): by changing source voltage in the basic configuration to 5 volts peak to peak, instead of 10 volts peak to peak, and keeping the rest. One sample is tested.
- Section 6.2.3 (changing wires length): by changing the Rip Cords length to 1 meter in the basic configuration, instead of 1.7 meter. Two samples are tested.
- Section 6.2.4 (changing load impedance): by changing the load impedance to  $9.815 \text{ k}\Omega$  in the basic configuration, instead of  $135.7 \Omega$ . One sample is tested.
- Section 6.2.5 (changing separation between wires): by changing the separation between Rip Cords to 1 cm (398.3 mils) in the basic configuration, instead of 0.24 cm (92.91 mils). Two samples are tested.

### 6.2.1 Basic Configuration

Figure 25, figure 29, figure 30, and figure 31 illustrate the main set up of the experiment. The following are the variables for this setup:

- Noise or source amplitude ( $V_s$ ): 10 volts peak to peak.
- Noise or source frequency ( $\omega = 2\pi f$ ): 100 kHz to 80 MHz.
- Rip Cords length ( $\lambda$ ): 1.7 m.
- Separation between Rip Cords (center to Center distance): 92.91 mils  $\approx$  .24 cm.
- Generator load impedance ( $Z_\lambda$ ): open or  $\infty$ .
- Generator source impedance ( $Z_S$ ): short or zero.
- Receptor load impedance ( $Z_{FE}$ ):  $135.7 \Omega$  parallel with  $2.2 \text{ M}\Omega$  and  $12 \text{ pF}$ .
- Receptor source impedance ( $Z_{NE}$ ):  $2.2 \text{ M}\Omega$  parallel with  $12 \text{ pF}$ .



The per unit length parameters of this configuration are computed both using methods 2 or 3 in chapter 4 and the above variables, the per unit length parameters are:

$$l_G = 0.895759 \mu H / m$$

$$l_M = 0.447880 \mu H / m$$

$$l_R = 0.636302 \mu H / m$$

$$c_M = 22.6001 pF / m$$

$$c_G = 29.0979 pF / m - c_M = 6.4978 pF / m$$

$$c_R = 45.2002 pF / m - c_M = 22.6001 pF / m$$

The objective is to predict the near-end and far-end voltages  $V_{NE} (\hat{V}_R(0))$  and  $V_{FE} (\hat{V}_R(\lambda))$  across the receptor circuit given the line cross-sectional dimensions, and the termination characteristics.

The experimental results are compared to the predictions of the model using **Tamer.m** over the frequency range of 100 kHz to 80 MHz in figure 32, figure 33, and figure 34 for three samples. The first figure of each sample provides both prediction of the model of  $V_{NE}$  (or  $\hat{V}_R(0)$ ) using equation 6.20, equation 6.23, and the experimental results, which is the voltage across the receptor source impedance. The second figure of each sample provides both prediction of the model of  $V_{FE}$  (or  $\hat{V}_R(\lambda)$ ) using equation 6.19, equation 6.22, and the experimental results, which is the voltage across the receptor load impedance.

Under these conditions, measurements are taken for three same samples: sample A, sample B, and sample C. The reason why we are dealing with three samples is only to make sure that the measurements are correct. Running the source file **Tamer.m** (**appendix A**) for the three samples A, B, and C are shown in figure 32, figure 33, and figure 34.

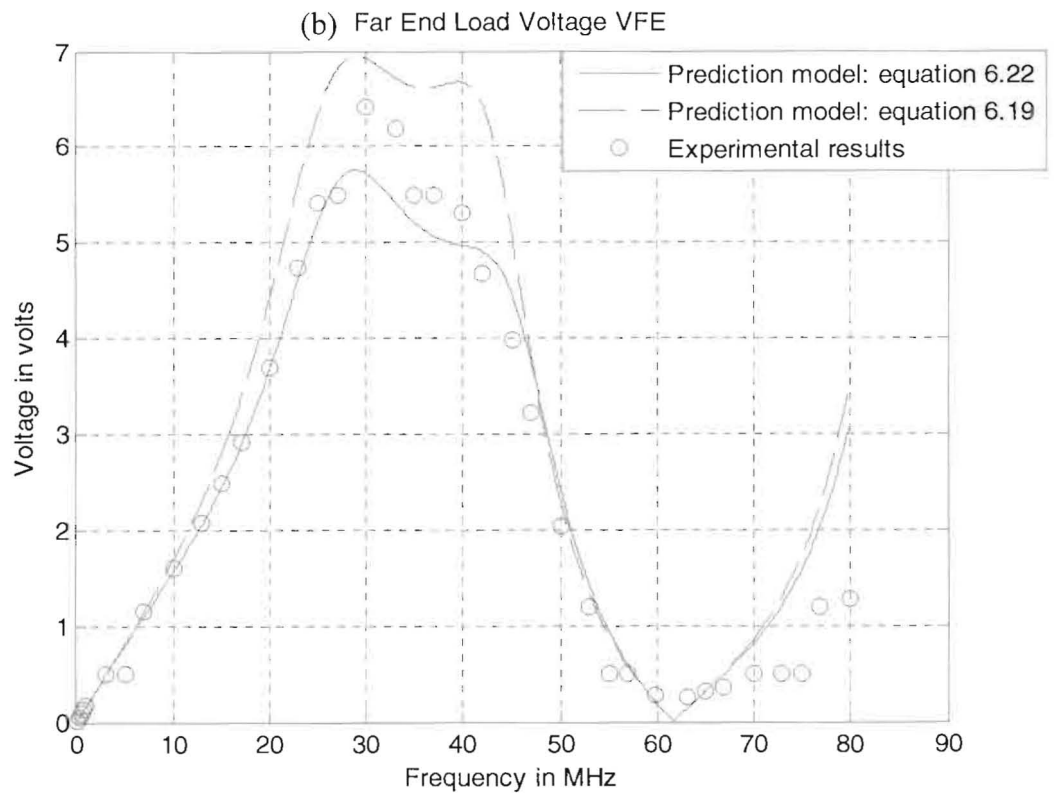
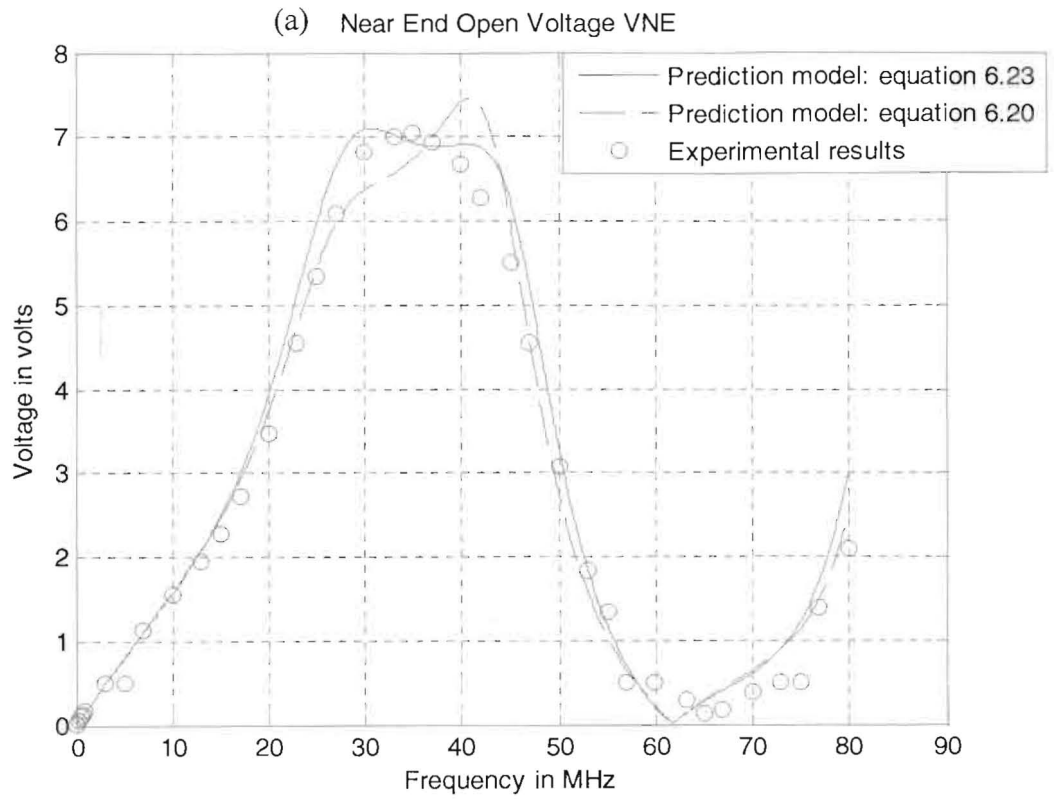


Figure 32: Basic configuration, sample A.

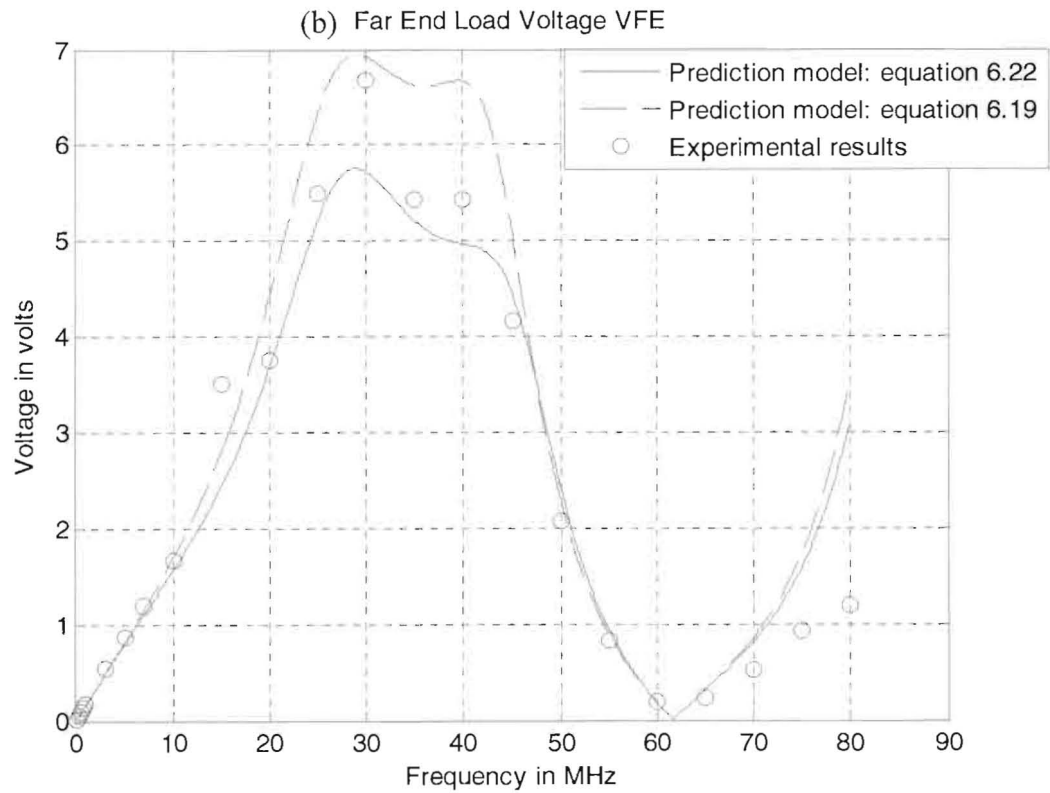
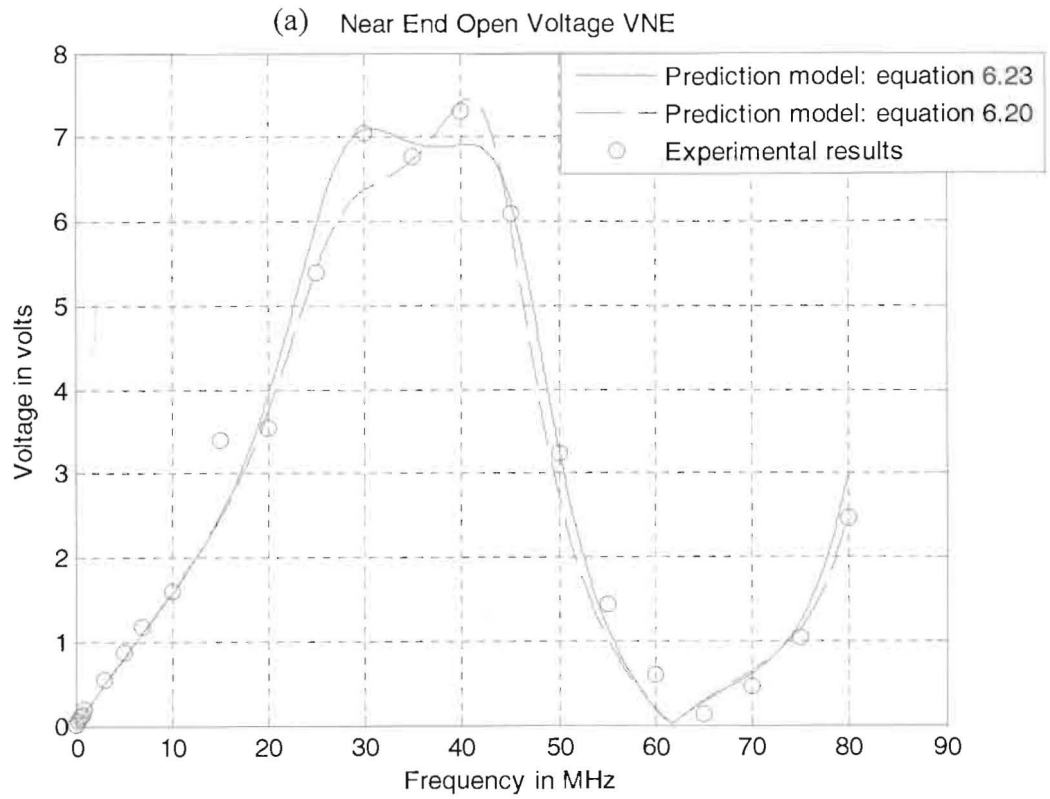


Figure 33: Basic configuration, sample B.

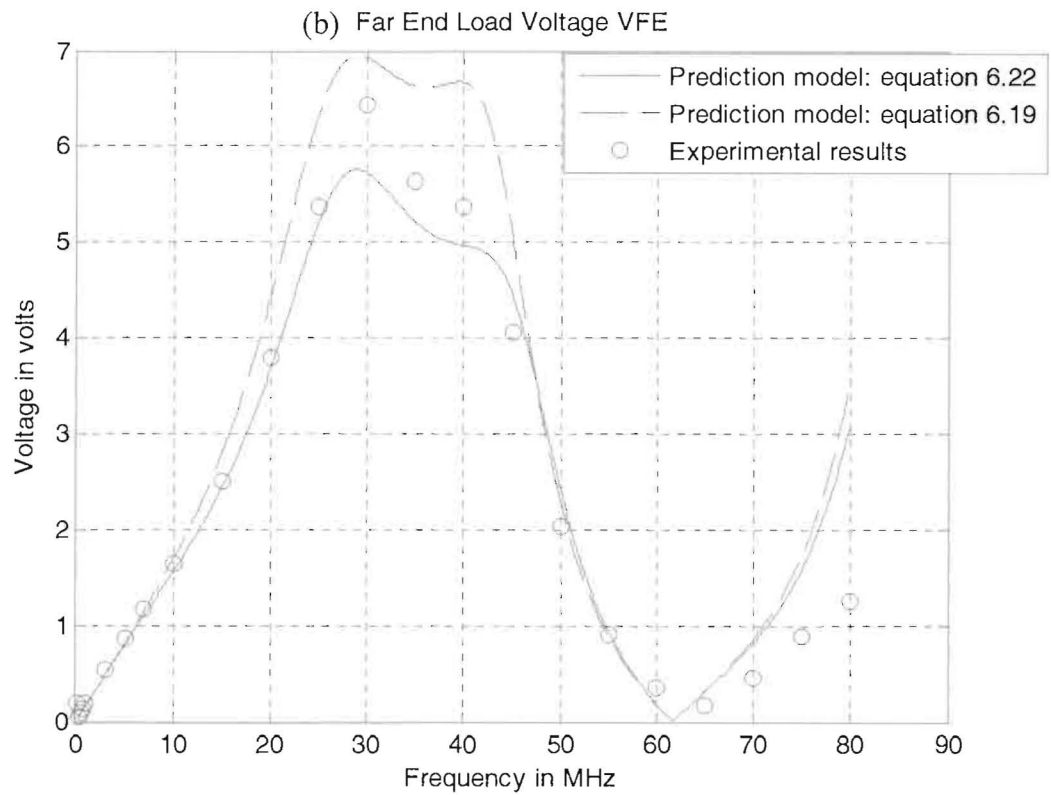
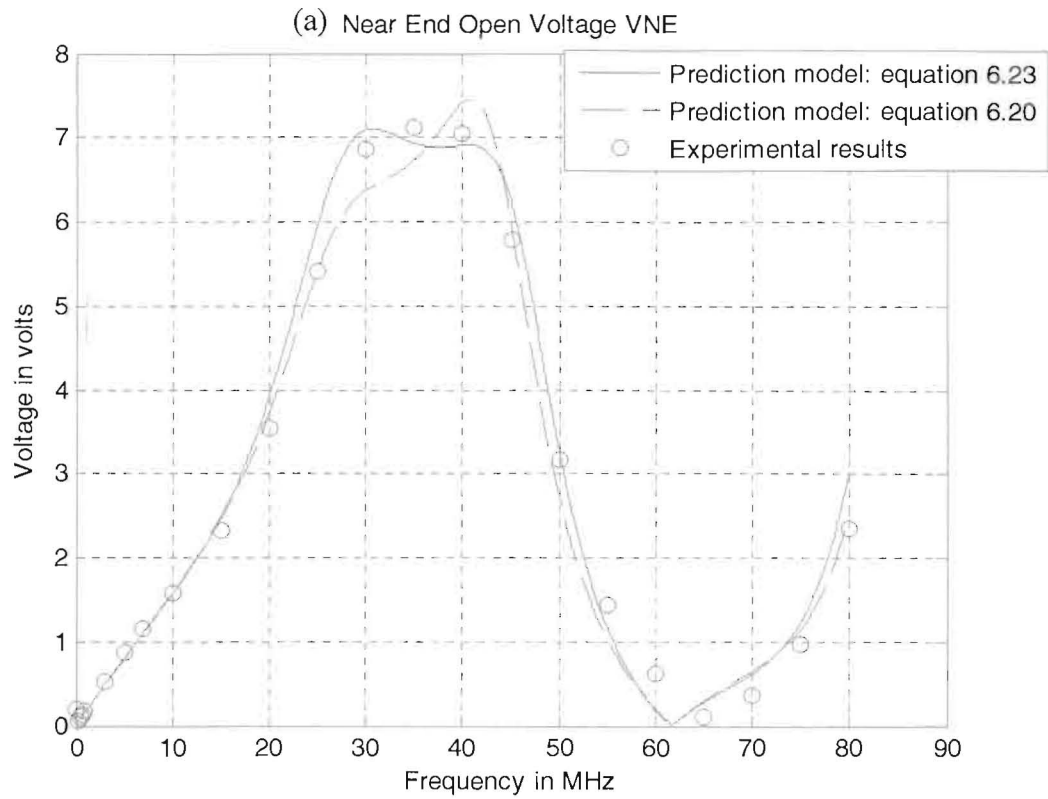


Figure 34: Basic configuration, sample C.

## 6.2.2 Changing Voltage Source Noise

In this section voltage source noise ( $V_s$ ) is changed in the basic configuration (section 6.2.1) to 5 volts peak to peak, instead of 10 volts peak to peak. One sample is tested. The following are the variables for this setup:

- Noise or source amplitude ( $V_s$ ): 5 volts peak to peak.
- Noise or source frequency ( $\omega = 2\pi f$ ): 100 kHz to 80 MHz.
- Rip Cords length ( $\lambda$ ): 1.7 m.
- Separation between Rip Cords (center to Center distance): 92.91 mils  $\approx$  .24 cm.
- Generator load impedance ( $Z_\lambda$ ): open or  $\infty$ .
- Generator source impedance ( $Z_S$ ): short or zero.
- Receptor load impedance ( $Z_{FE}$ ): 135.7  $\Omega$  parallel with 2.2  $M\Omega$  and 12 pF .
- Receptor source impedance ( $Z_{NE}$ ): 2.2  $M\Omega$  parallel with 12 pF .

The per unit length parameters of this configuration are computed and are resulted as same as of the basic configuration.

The objective is to predict the near-end and far-end voltages  $V_{NE}$  ( $\hat{V}_R(0)$ ) and  $V_{FE}$  ( $\hat{V}_R(\lambda)$ ) across the receptor circuit given the line cross-sectional dimensions, and the termination characteristics.

The experimental results are compared to the predictions of the model using **Tamer.m** over the frequency range of 100 kHz to 80 MHz in figure 35. The first figure provides both prediction of the model of  $V_{NE}$  (or  $\hat{V}_R(0)$ ) using equation 6.20, equation 6.23, and the experimental results, which is the voltage across the receptor source impedance. The second figure provides both prediction of the model of  $V_{FE}$  (or  $\hat{V}_R(\lambda)$ ) using equation 6.19, equation 6.22, and the experimental results, which is the voltage across the receptor load impedance. Running the source file **Tamer.m (appendix A)** is shown in figure 35.

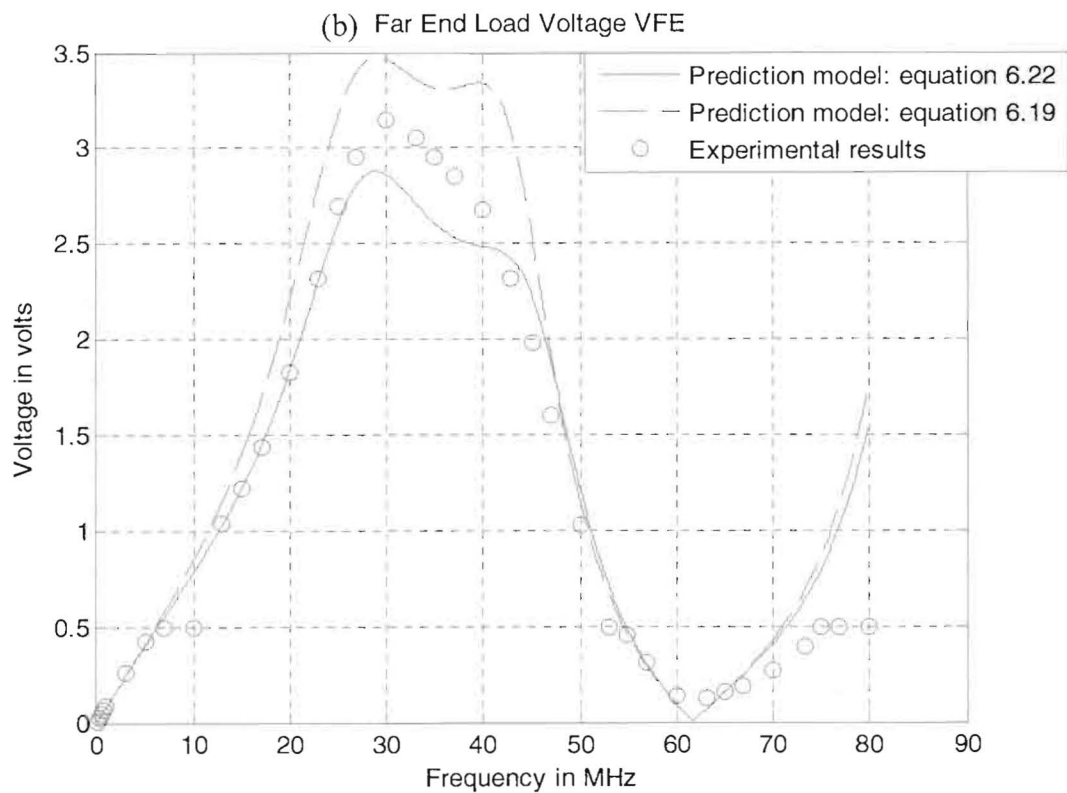
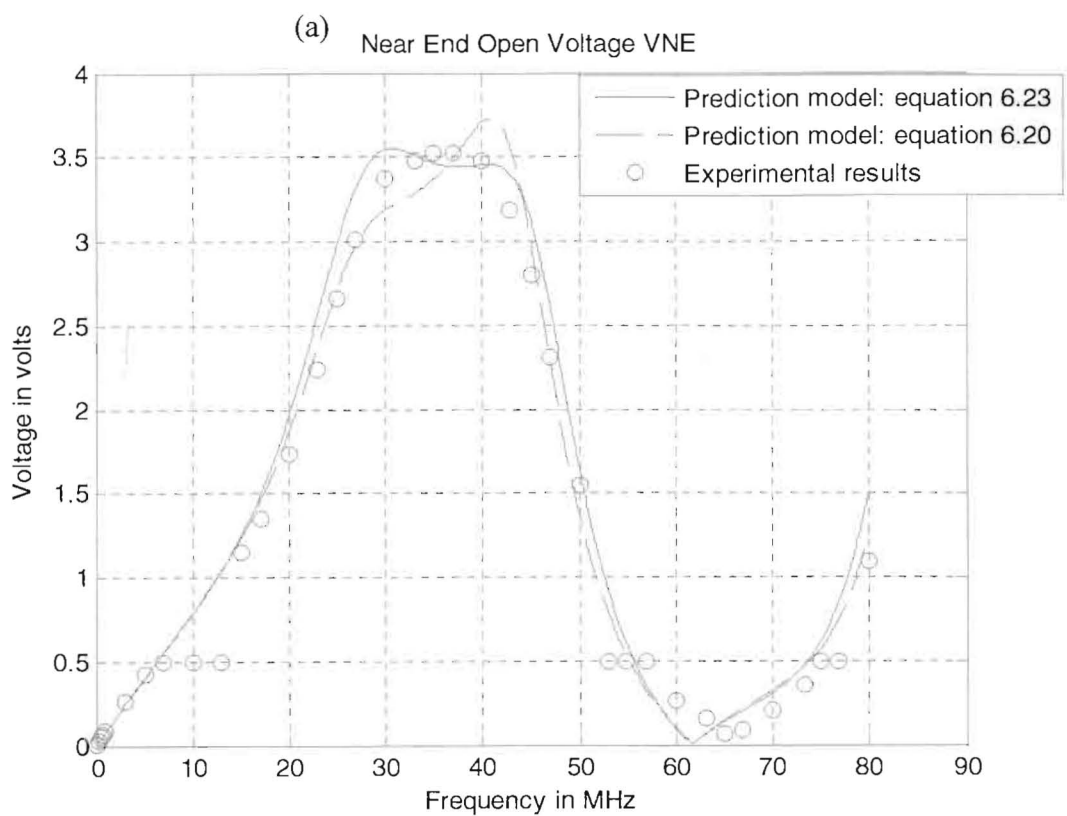


Figure 35: Changing voltage source noise to 5 volts peak to peak.

### 6.2.3 Changing Wires Length

In this section Rip Cords length ( $\lambda$ ) is changed in the basic configuration (section 6.2.1) to 1 meter, instead of 1.7 meter. Two samples are tested. The following are the variables for this setup:

- Noise or source amplitude ( $V_s$ ): 10 volts peak to peak.
- Noise or source frequency ( $\omega = 2\pi f$ ): 100 kHz to 80 MHz.
- Rip Cords length ( $\lambda$ ): 1.0 m.
- Separation between Rip Cords (center to Center distance): 92.91 mils  $\approx$  .24 cm.
- Generator load impedance ( $Z_\lambda$ ): open or  $\infty$ .
- Generator source impedance ( $Z_S$ ): short or zero.
- Receptor load impedance ( $Z_{FE}$ ): 135.7  $\Omega$  parallel with 2.2  $M\Omega$  and 12 pF .
- Receptor source impedance ( $Z_{NE}$ ): 2.2  $M\Omega$  parallel with 12 pF .

The per unit length parameters of this configuration are computed and are resulted as same as of the basic configuration.

The objective is to predict the near-end and far-end voltages  $V_{NE}$  ( $\hat{V}_R(0)$ ) and  $V_{FE}$  ( $\hat{V}_R(\lambda)$ ) across the receptor circuit given the line cross-sectional dimensions, and the termination characteristics.

The experimental results are compared to the predictions of the model using **Tamer.m** over the frequency range of 100 kHz to 80 MHz in figure 36, and figure 37 for two samples. The first figure of each sample provides both prediction of the model of  $V_{NE}$  (or  $\hat{V}_R(0)$ ) using equation 6.20, equation 6.23, and the experimental results, which is the voltage across the receptor source impedance. The second figure of each sample provides both prediction of the model of  $V_{FE}$  (or  $\hat{V}_R(\lambda)$ ) using equation 6.19, equation 6.22, and the experimental results, which is the voltage across the receptor load impedance. Under these conditions, measurements are taken for two samples: sample A, and sample B. The reason why we are dealing with two samples is only to make sure that the measurements are correct. Running the source file **Tamer.m** (appendix A) for the two samples A, and B are shown in figure 36, and figure 37.

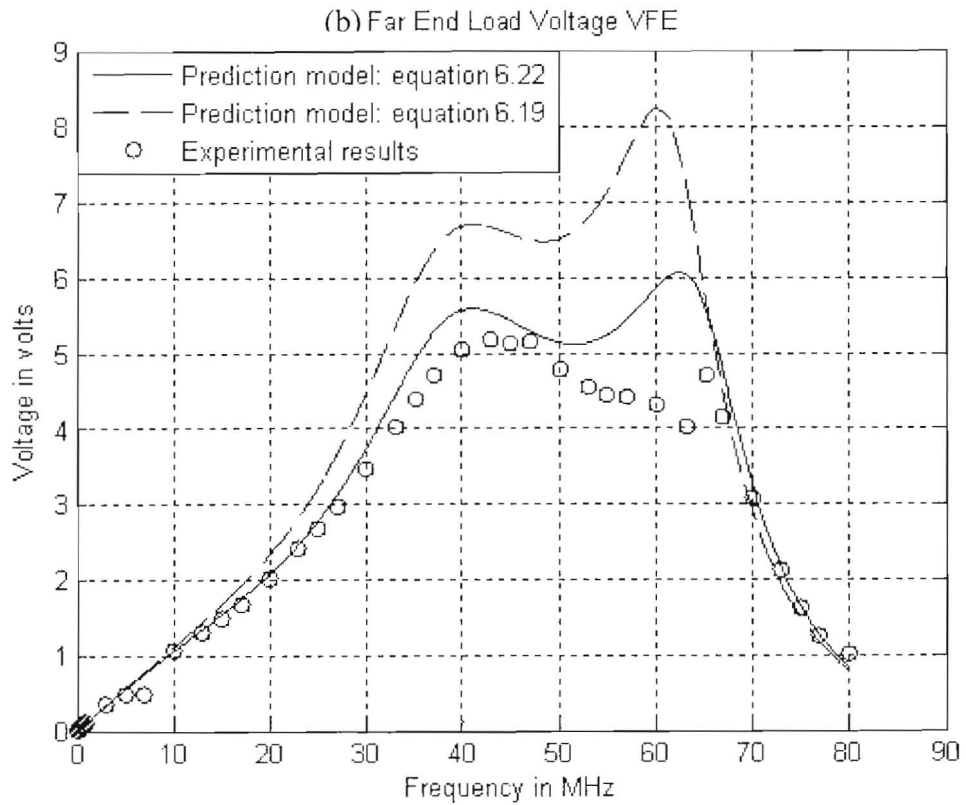
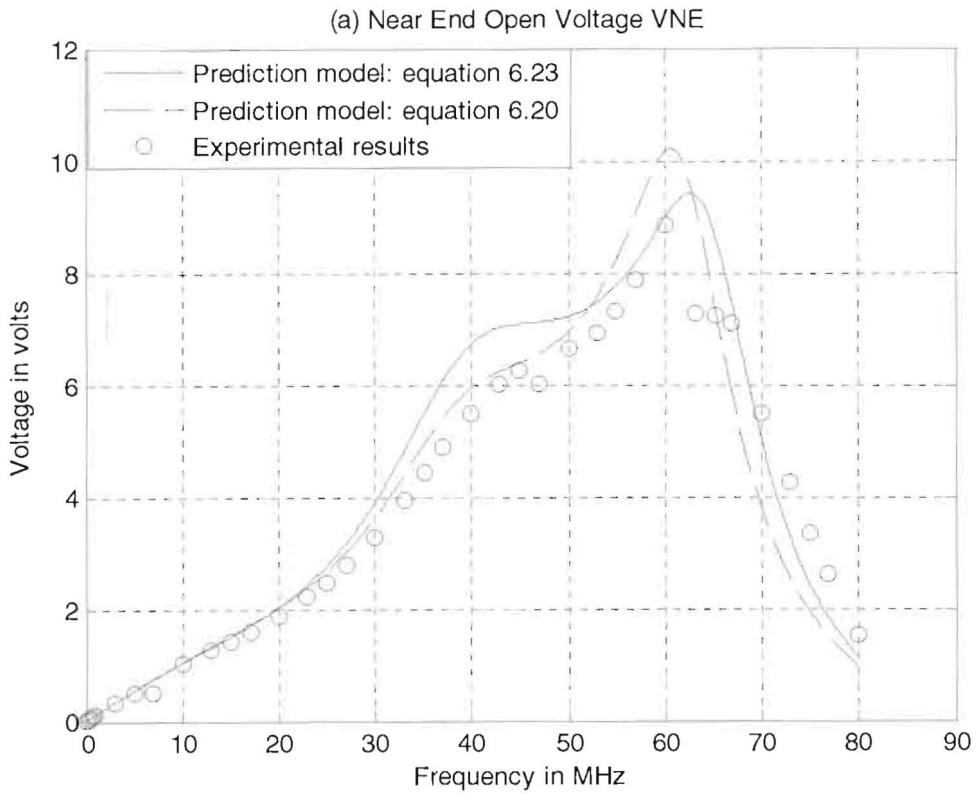


Figure 36: Changing wires length to 1.0 meter, sample A.



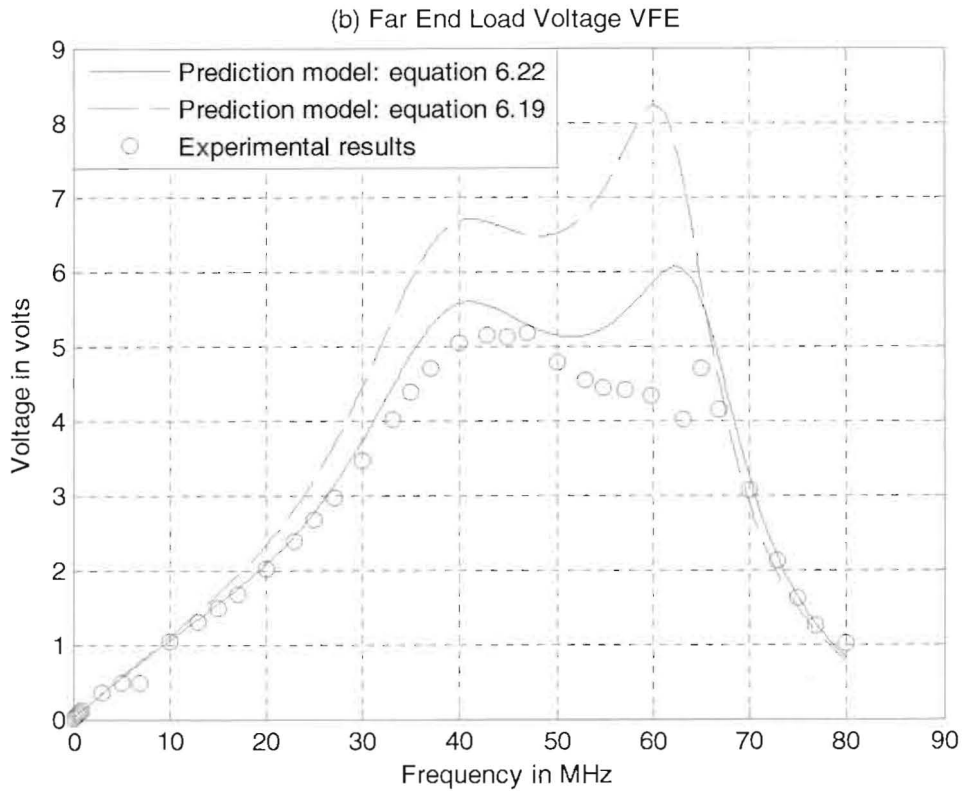
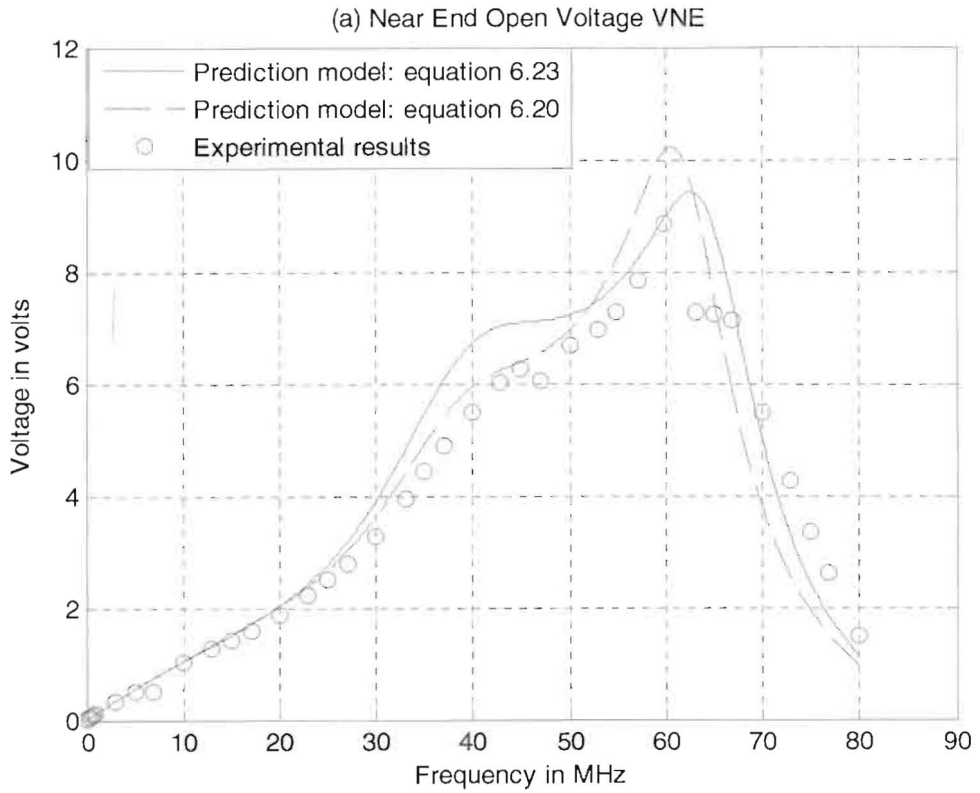


Figure 37: Changing wires length to 1.0 meter, sample B.

## 6.2.4 Changing Load Impedance

In this section load impedance ( $Z_{FE}$ ) is changed in the basic configuration (section 6.2.1) to  $9.851\text{ k}\Omega$ , instead of  $135.7\ \Omega$ . One sample is tested. The following are the variables for this setup:

- Noise or source amplitude ( $V_s$ ): 10 volts peak to peak.
- Noise or source frequency ( $\omega = 2\pi f$ ): 100 kHz to 80 MHz.
- Rip Cords length ( $\lambda$ ): 1.7 m.
- Separation between Rip Cords (center to Center distance): 92.91 mils  $\approx$  .24 cm.
- Generator load impedance ( $Z_\lambda$ ): open or  $\infty$ .
- Generator source impedance ( $Z_S$ ): short or zero.
- Receptor load impedance ( $Z_{FE}$ ):  $9.851\text{ k}\Omega$  parallel with  $2.2\text{ M}\Omega$  and  $12\text{ pF}$ .
- Receptor source impedance ( $Z_{NE}$ ):  $2.2\text{ M}\Omega$  parallel with  $12\text{ pF}$ .

The per unit length parameters of this configuration are computed and are resulted as same as of the basic configuration.

The objective is to predict the near-end and far-end voltages  $V_{NE}$  ( $\hat{V}_R(0)$ ) and  $V_{FE}$  ( $\hat{V}_R(\lambda)$ ) across the receptor circuit given the line cross-sectional dimensions, and the termination characteristics.

The experimental results are compared to the predictions of the model using **Tamer.m** over the frequency range of 100 kHz to 80 MHz in figure 38. The first figure provides both prediction of the model of  $V_{NE}$  (or  $\hat{V}_R(0)$ ) using equation 6.20, equation 6.23, and the experimental results, which is the voltage across the receptor source impedance. The second figure provides both prediction of the model of  $V_{FE}$  (or  $\hat{V}_R(\lambda)$ ) using equation 6.19, equation 6.22, and the experimental results, which is the voltage across the receptor load impedance. Running the source file **Tamer.m** (appendix A) is shown in figure 38. Experimentally, the function generator does not apply more than 3 volts peak to peak around 30 and 50 MHz because the circuit sinks more current source and these results experimentally around 30 volts at both receptor circuit terminals [16][15].

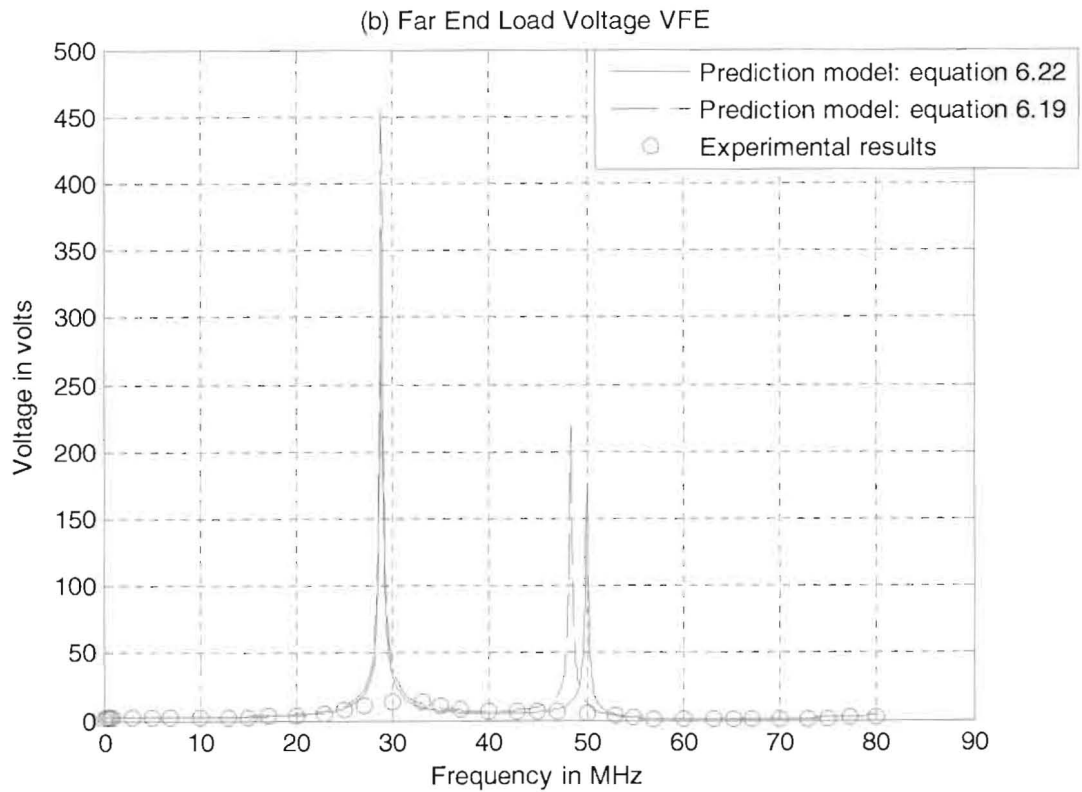
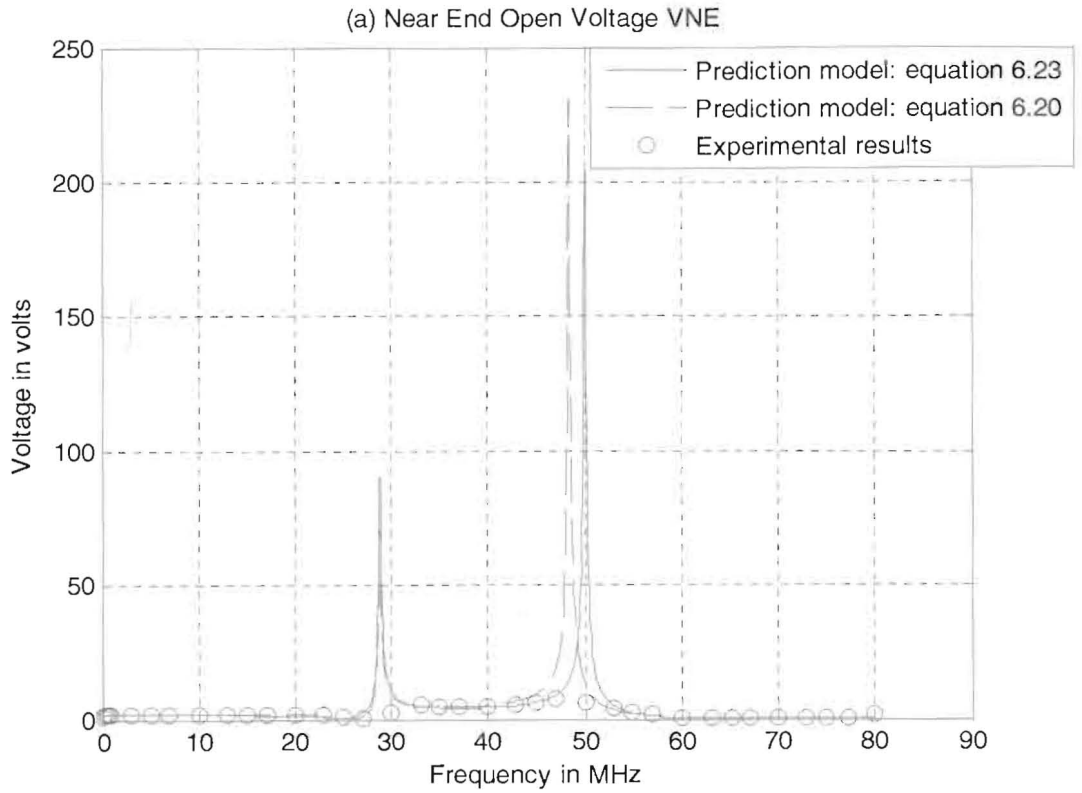


Figure 38: Changing Load Impedance to 9.851 k $\Omega$  .

## 6.2.5 Changing Separation between Wires

In this section separation between Rip Cords (center to Center distance) is changed in the basic configuration (section 6.2.1) to 1 cm (398.3 mils), instead of 0.24 cm (92.91 mils). Two samples are tested. The following are the variables for this setup:

- Noise or source amplitude ( $V_s$ ): 10 volts peak to peak.
- Noise or source frequency ( $\omega = 2\pi f$ ): 100 kHz to 80 MHz.
- Rip Cords length ( $\lambda$ ): 1.7 m.
- Separation between Rip Cords (center to Center distance): 1 cm (398.3 mils).
- Generator load impedance ( $Z_\lambda$ ): open or  $\infty$ .
- Generator source impedance ( $Z_S$ ): short or zero.
- Receptor load impedance ( $Z_{FE}$ ):  $135.7 \Omega$  parallel with  $2.2 M\Omega$  and  $12 \text{ pF}$ .
- Receptor source impedance ( $Z_{NE}$ ):  $2.2 M\Omega$  parallel with  $12 \text{ pF}$ .

The per unit length parameters for this configuration were computed (it is different than the previous one) either using methods 2 or 3 in chapter 4 as:

$$l_G = 1.51169 \mu\text{H} / \text{m}$$

$$l_M = 0.755846 \mu\text{H} / \text{m}$$

$$l_R = 1.23536 \mu\text{H} / \text{m}$$

$$c_M = 7.83763 \text{ pF} / \text{m}$$

$$c_G = 12.3955 \text{ pF} / \text{m} - c_M = 4.55787 \text{ pF} / \text{m}$$

$$c_R = 15.6753 \text{ pF} / \text{m} - c_M = 7.83767 \text{ pF} / \text{m}$$

The inductance and capacitance matrices are given by:

$$\bar{L} = \begin{bmatrix} l_G & l_M \\ l_M & l_R \end{bmatrix} = \begin{bmatrix} 1.51169 \mu\text{H} / \text{m} & 0.755846 \mu\text{H} / \text{m} \\ 0.755846 \mu\text{H} / \text{m} & 1.23536 \mu\text{H} / \text{m} \end{bmatrix}$$

$$\bar{C} = \begin{bmatrix} c_G + c_M & -c_M \\ -c_M & c_R + c_M \end{bmatrix} = \begin{bmatrix} 12.3955 \text{ pF} / \text{m} & -7.83763 \text{ pF} / \text{m} \\ -7.83763 \text{ pF} / \text{m} & 15.6753 \text{ pF} / \text{m} \end{bmatrix}$$

The objective is to predict the near-end and far-end voltages  $V_{NE}$  ( $\hat{V}_R(0)$ ) and  $V_{FE}$  ( $\hat{V}_R(\lambda)$ ) across the receptor circuit given the line cross-sectional dimensions, and the termination characteristics.

The experimental results are compared to the predictions of the model using **Tamer.m** over the frequency range of 100 kHz to 80 MHz in figure 39, and figure 40 for two samples. The first figure of each sample provides both prediction of the model of  $V_{NE}$  (or  $\hat{V}_R(0)$ ) using equation 6.20, equation 6.23, and the experimental results, which is the voltage across the receptor source impedance. The second figure of each sample provides both prediction of the model of  $V_{FE}$  (or  $\hat{V}_R(\lambda)$ ) using equation 6.19, equation 6.22, and the experimental results, which is the voltage across the receptor load impedance.

Under these conditions, measurements are taken for two same samples: sample A, and sample B. The reason why we are dealing with two samples is only to make sure that the measurements are correct. Running the source file **Tamer.m (appendix A)** for the two samples A, and B are shown in figure 39, and figure 40.

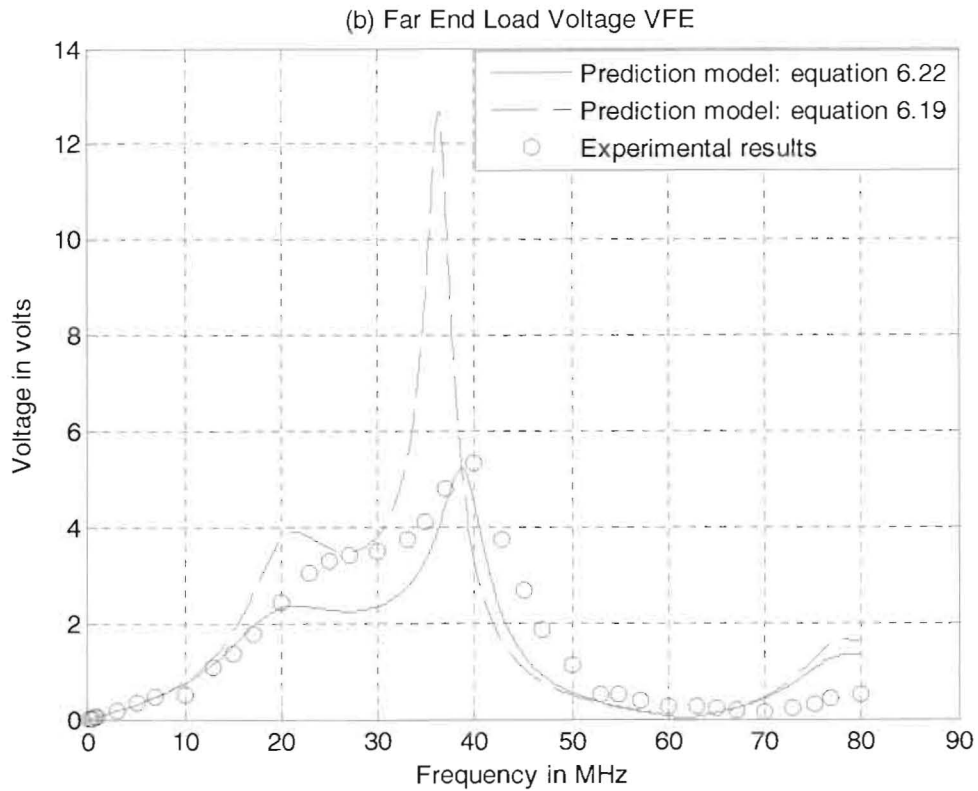
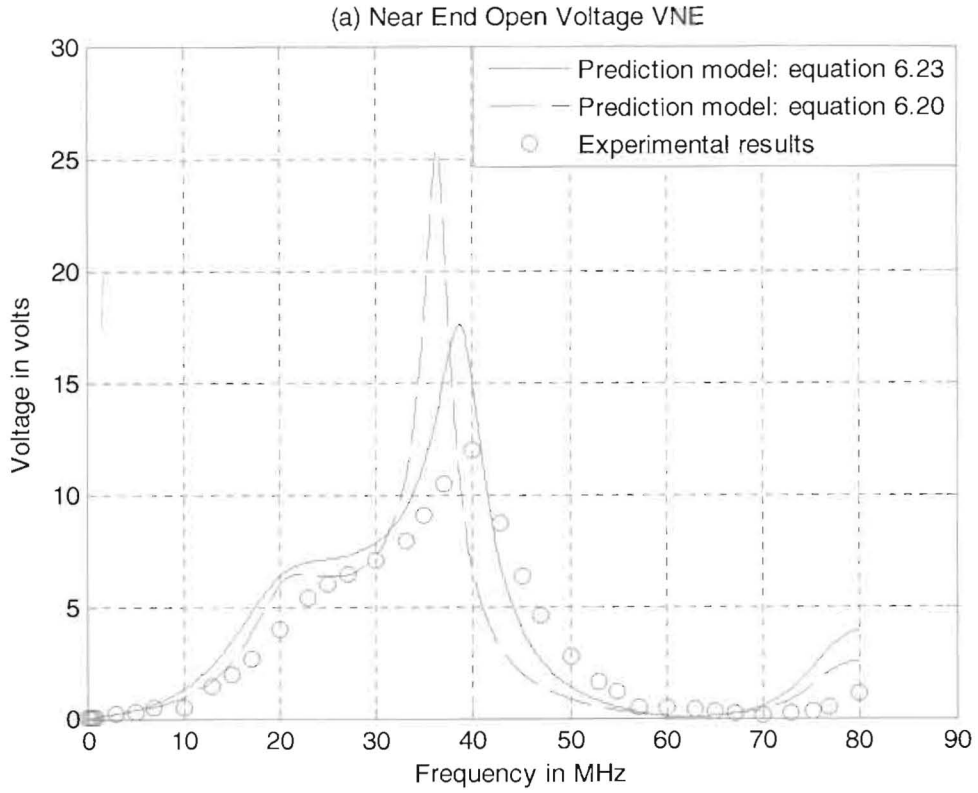


Figure 39: Changing separation between wires to 1 cm (398.3 mils), sample A.

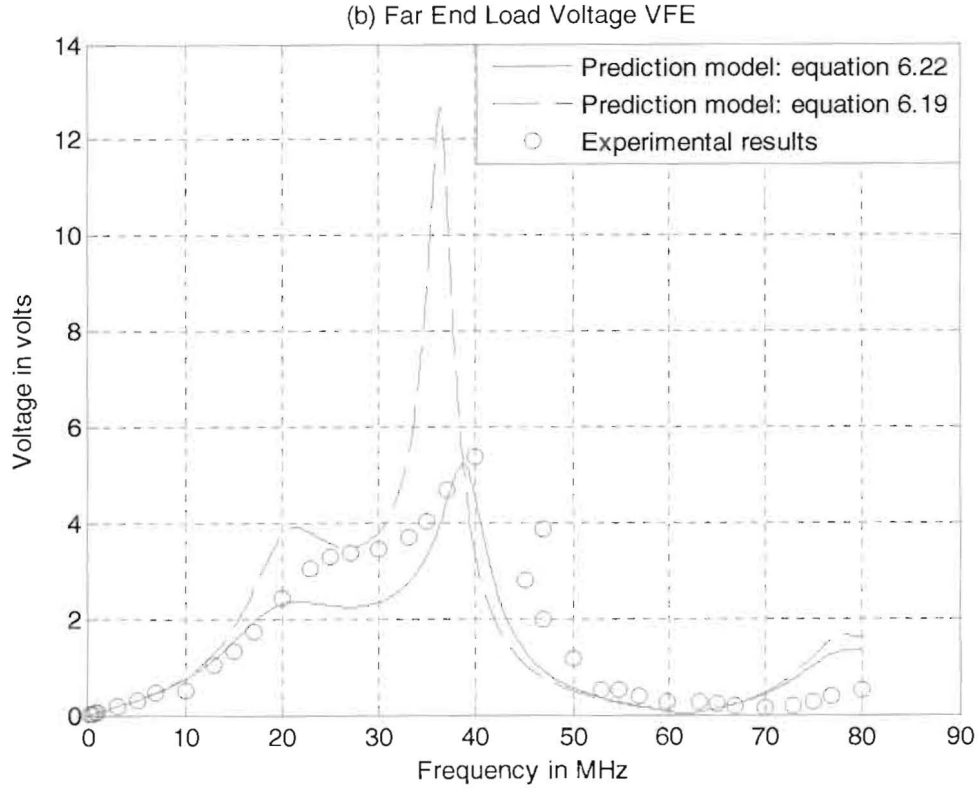
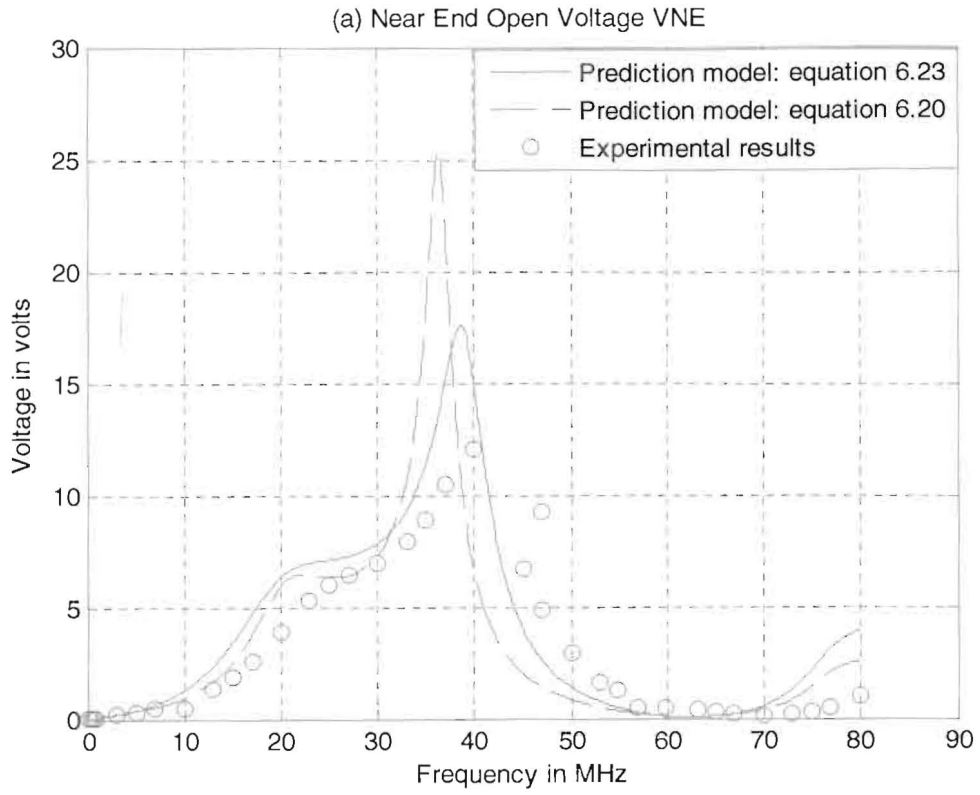


Figure 40: Changing separation between wires to 1 cm (398.3 mils), sample B.

# CHAPTER SEVEN

## CONCLUSION

In order to say that a design has been considered as a model, the theoretical predictions should meet quite enough the practical or experimental measurements – under specific circumstances, variables, and assumptions.

A model to predict Electromagnetic Interference in Automotive Data Communication Structure was derived. The results and predictions agreed. To be able to predict the signal at the victim circuit, we need to go over the following three steps:

- The per unit length parameters should be determined.
- The equations for multi-transmission lines have to be solved.
- The terminal constraints should be substituted in the main equations to determine the unknown coefficients.

It's important to mention that the model depends on the following assumptions,

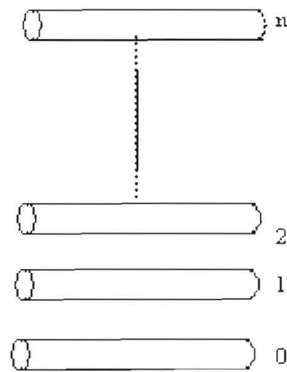
- The wires are symmetric and parallel,
- The wires and the surrounding medium are lossless.
- The medium is homogeneous with  $\epsilon_r = 3.4$ .
- The source signals are sinusoids.

The model predicts interference by varying the following parameters:

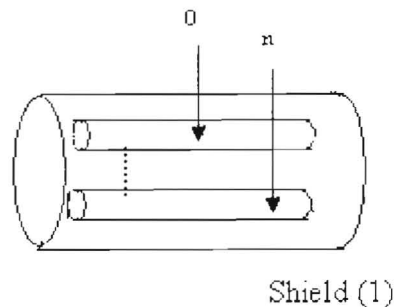
- Frequency up to 80MHz.
- Source and/or load voltages.
- Source and/or load impedances.
- Number of wires.
- The circuit length.
- Uniform wire separation.
- Dielectric material.
- Insulation thickness.
- Wire radius.
- The reference wire.



The results presented in this thesis indicate that the further steps can be done by increasing the frequency up to 1 GHz, including the resistance and conductance matrices, testing the wires under non-homogenous medium, and measuring the per unit length parameters for cross wires.



(a)



(b)

Figure 41: Multi-transmission lines examples, (a)  $n$  wires above a ground plane, (b) untwisted shielded pair.

Figure 41 illustrates examples of multi-transmission lines (MTL) that can be tested and modeled in the future. Future work can be done by applying typical applications as circuits of  $n$  wires,  $n$  wires above a ground plane, UTP (unshielded twisted pair), STP (shielded twisted pair), and coaxial cables.

# APPENDIX A

## MATLAB SOURCE CODE

This appendix describes a MATLAB computer program for computing the interference between three adjacent circuits (multi-transmission lines). The source code is **Tamer.m**.

The source code was written using MATLAB editor and saved as **Tamer.m**. The program was tested and compiled with MATLAB version 7.2.0.232(R2006a). The user needs to input the measured value of his/her experiments. The source code reads the inputs, computes the interference, and draws the figures. The code falls into two distinct categories: one which computes the far end voltages of the receptor circuit  $V_{FE}$  (or  $\hat{V}_R(\lambda)$ ) and plots the computed results versus the measured results and one which computes the near end voltages of the receptor circuit  $V_{NE}$  (or  $\hat{V}_R(0)$ ) and plots the computed results versus the measured results. The following is an example of running the source code in MATLAB of figure 33:

```
>> Tamer
```

```
Please enter the peak to peak measured voltages in volts at the load side (VFE or Vr(l))[0.04 0.11 0.18 0.26 0.3672 1 1 2.3145 3.223 4.148 4.961 5.83 7.373 9.463 10.84 11 12.832 12.363 11 11 10.625 9.346 7.969 6.465 4.063 2.406 1 1 0.5322 0.498 0.626 0.7285 1 1 1 2.402 2.551 ]
```

```
Please enter the peak to peak measured voltages i volts at the source side(VNE or Vr(0))[0.04 0.11 0.19 0.26 0.3699 1 1 2.2754 3.105 3.91 4.555 5.47 6.934 9.092 10.684 12.168 13.633 14.004 14.082 13.88 13.379 12.539 10.996 9.102 6.147 3.664 2.676 1 1 0.6025 0.2551 0.3301 0.7891 1 1 2.766 4.18 ]
```

```
Please enter the peak to peak measured voltage in volts from the function generator  
10
```

```
Please enter the operating frequencies in Hertz [100000 300000 500000 699300 1000000 3003000 5000000 6993000 10000000 12980000 14970000 17007000 20000000 22989000 25000000 27030000 30030000 33110000 34970000 36969000 40000000
```

42010000 45050000 47060000 50000000 53050000 55100000 56980000 59880000  
63090000 64940000 66890000 69930000 72990000 74910000 76920000 80000000]

**Please enter the per unit length generator inductance (H/meter)  $8.95759 \times 10^{-07}$**

**Please enter the per unit length mutual inductance (H/meter)  $4.47880 \times 10^{-07}$**

**Please enter the per unit length receptor inductance (H/meter)  $6.36302 \times 10^{-07}$**

**Please enter the per unit length mutual capacitance (F/meter)  $2.26001 \times 10^{-11}$**

**Please enter the per unit length generator capacitance added to the mutual capacitance (F/meter)  $2.90979 \times 10^{-11}$**

**Please enter the per unit length receptor capacitance added to the mutual capacitance (F/meter)  $4.52002 \times 10^{-11}$**

**Please enter the impedance at load end (ZFE or far end)(Ohm) 135.7**

**Please enter the Rip Cords length (meter) 1.7**

>>

The results are plotted as in figure 33. The source code of **Tamer.m** is written below:

```
%Youngstown State University
%Done by: Tamer A. Taher
%Electrical and Computer Engineering Department
%Youngstown, OH 44555
%This source code calculates the voltage at the far end and near end of
%three Rip Cord wires as shown in figure 25 in my thesis
clear all;
format long e;
APL1= input('Please enter the peak to peak measured voltages in volts
at the load side (VFE or Vr(1))');
AP01= input('Please enter the peak to peak measured voltages i volts at
the source side(VNE or Vr(0))');
Vinn1= input('Please enter the peak to peak measured voltage in volts
from the function generator');
FREQUENCYH = input('Please enter the operating frequencies in Hertz');
LG= input('Please enter the per unit length generator inductance
(H/meter)');
LM= input('Please enter the per unit length mutual inductance
(H/meter)');
LR= input('Please enter the per unit length receptor inductance
(H/meter)');
CM= input('Please enter the per unit length mutual capacitance
(F/meter)');
CG1= input('Please enter the per unit length generator capacitance
added to the mutual capacitance (F/meter)');
CR1= input('Please enter the per unit length receptor capacitance added
to the mutual capacitance (F/meter)');
R= input('Please enter the impedance at load end (ZFE or far end)(Ohm)
');
L= input('Please enter the Rip Cords length(meter)');
APL=APL1/2;
```



```

m=m+1;
end
ff=FREQUENCYq/((10^6*2*pi));
ff1=FREQUENCY/((10^6*2*pi));
figure
plot(ff,VNE,'-k',ff,VRO1,'--k')
hold on
plot(ff1,APO,'ko')
title(' (a) Near End Open Voltage VNE')
ylabel('Voltage in volts')
xlabel('Frequency in MHz')
grid on
h = legend('Prediction model: equation 6.23','Prediction model:
equation 6.20','Experimental results',2);
set(h,'Interpreter','none')
figure
plot(ff,VFE,'-k',ff,VRL1,'--k')
hold on
plot(ff1,APL,'ko')
title(' (b) Far End Load Voltage VFE')
ylabel('Voltage in volts')
xlabel('Frequency in MHz')
grid on
h = legend('Prediction model: equation 6.22','Prediction model:
equation 6.19','Experimental results',2);
set(h,'Interpreter','none')

```

## REFERENCES

1. Matthew M. Radmanesh, "Radio Frequency and Microwave Electronics Illustrated", Upper Saddle River, NJ, Prentice Hall PTR, 2001.
2. Niels Faché, Frank Olyslager, and Daniël De Zutter, "Electromagnetic and Circuit Modeling of Multiconductor Transmission Lines", Oxford University Press, 1993.
3. M.S. Nakhla and Q.J. Zhang, "Modeling and Simulation of High Speed VLSI Interconnects", Boston Kluwer Academic Publishers, 1994.
4. Clayton R. Paul, "Analysis of Multiconductor Transmission Lines", New York: Wiley, 1994.
5. Clayton R. Paul, "Introduction to Electromagnetic Compatibility", Hoboken, N.J. Wiley-Interscience, 2006, 2<sup>nd</sup> ed.
6. Henry W. Ott, "Noise Reduction Techniques in Electronic Systems" New York: Wiley, 1988, 2<sup>nd</sup> ed.
7. Constantine A. Balanis, "Antenna Theory: Analysis and Design", John Wiley, 2005, 3<sup>rd</sup> ed.
8. Reinhold Ludwig and Pavel Bretchko, "RF Circuit Design: Theory and Applications", Upper Saddle River, NJ: Prentice-Hall, c2000.
9. C. R. Paul and J.A. McKnight, "Prediction of Crosstalk Involving Twisted Pairs of Wires, Part II, A Simplified, Low-Frequency Prediction Model", *IEEE Trans. on Electromagnetic Compatibility*, Vol. EMC-21, No. 2, pp. 105-114, May 1979.
10. C. R. Paul, "Computation of Crosstalk in a Multiconductor Transmission Line", *IEEE Trans. on Electromagnetic Compatibility*, Vol. EMC-23, No. 4, pp. 352-358, Nov 1981.
11. C. R. Paul, "On the Superposition of Inductive and Capacitive Coupling in Crosstalk Prediction Models", *IEEE Trans. on Electromagnetic Compatibility*, Vol. EMC-24, No. 3, pp. 335-343, Aug 1982.
12. C. R. Paul, "A SPICE Model for Multiconductor Transmission Lines Excited by an Incident Electromagnetic Field," *IEEE Trans. on Electromagnetic Compatibility*, Vol. EMC-36, No. 4, pp.342-354, Nov 1994.

13. C. R. Paul, "Estimation of Crosstalk in Three-Conductor Transmission Lines", *IEEE Trans. on Electromagnetic Compatibility*, Vol. EMC-26, No. 4, Nov 1984.
14. C. R. Paul, "Useful Matrix Chain Parameter Identities for the Analysis of Multiconductor Transmission Lines", *IEEE Trans. on Microwave Theory and Techniques*, Vol. MTT-23, No. 9, pp. 756-760, Sep 1975.
15. C. R. Paul, "Solution of the Transmission Line Equations for Three-Conductor Lines in Homogeneous Media", *IEEE Trans. on Electromagnetic Compatibility*, Vol. EMC-20, No. 1, pp. 216-222, Feb 1978.
16. C. R. Paul, "Prediction of Crosstalk in Ribbon Cables: Comparison of Model Predictions and Experiment Results", *IEEE Trans. on Electromagnetic Compatibility*, Vol. EMC-20, No. 3, pp. 394-406, Aug 1978.
17. [www.noiseken.com](http://www.noiseken.com). MODEL WST-2001, access date: Dec 1<sup>st</sup>, 2006.